Electronic Journal of Qualitative Theory of Differential Equations
2025, No. **32**, 1–41; https://doi.org/10.14232/ejqtde.2025.1.32 www.math.u-szeged.hu/ejqtde/

Dynamic behavior of a stochastic fast-slow fishery economic model with Allee effect

Xiaoqi Han and **Yue Zhang** ✉

College of Sciences, Northeastern University, Shenyang, Liaoning province, 110819, P.R. China

Received 7 November 2024, appeared 3 July 2025
Communicated by Michal Fečkan

Abstract. This article investigates a stochastic fast-slow fishery economic model with Allee effect. The fast-slow dynamic behavior of the deterministic system is discussed by using the theory of singular perturbation. Research shows that singular Hopf bifurcations will occur under the influence of strong Allee effect, while the dynamic behavior of the system will be more complex under the influence of weak Allee effect, resulting in relaxation oscillations. For the stochastic system, the existence of stationary distribution is discussed for both stochastic fast-slow system and system with time scale parameter as ordinary parameter. Then, the stochastic bifurcation behavior of the system is discussed, and it is found that stochastic-P bifurcation and stochastic-D bifurcation will occur. Finally, the correctness of the conclusion is verified through numerical simulation.

Keywords: fast-slow system, canard circle, relaxation oscillation, ergodic stationary distribution, stochastic bifurcation.

2020 Mathematics Subject Classification: 34E13, 34C26, 34C23, 34E15, 34E17, 37H20, 37H30.

1 Introduction

The bioeconomic model of fishery resources is based on the dynamic model of fishery populations, combined with ecological, economic and social factors, to study the relationship between the quantity of fishery resources and human activities. The fishing industry has high social significance, as it directly affects the livelihoods and food supply of fishermen. In order to ensure the stable growth of human needs, it is necessary to study the stability of the dynamic model of fishing resources [20, 34].

In the fishery economy, the human capture operations are a key link and the main way to obtain fishery resources, driving the development of the fishery economy. In recent years, many scholars have incorporated capture as a parameter into biological models, studied bioeconomic models described by differential algebraic equations, and generated interesting and rich dynamic behaviors [2, 15, 25]. Clark [7] incorporated dynamic capture into the model,

✉Corresponding author. Email: zhangyue@mail.neu.edu.cn

believing that capture would be affected by total revenue and total cost, and treating it as a fixed parameter is unrealistic. Therefore, it is necessary to introduce capture as a variable into the bioeconomic system.

The Allee effect is an important dynamic phenomenon in ecosystems [18], which suggests that when a population is too sparse or too dense, it can inhibit population growth, meaning that each population has its own optimal density for survival. With the deepening of research on population dynamics, scholars have gradually introduced the classification of strong and weak Allee effects in order to more accurately describe the performance of populations under different degrees of low density. For species with strong Allee effect [35], once the population drops to the critical density, the species is likely to become extinct. For species under weak Allee effect [11], when the species density is low, they still have a certain degree of self-sustaining ability, which means that even if the species density is small, they can naturally grow to a certain extent. Understanding and considering the Allee effect is crucial for sustainable fishing in the fishery economy. Considering the Allee effect can help fishery managers develop reasonable fishing quotas and fishing bans to ensure the health of fish populations and the sustainable use of fishery resources. Lin [23] studied a single-species logistic model incorporating the Allee effect and explored how the Allee effect impacts species stability and extinction risk. Ashutosh [27] developed a fish capture model with logistic growth and Allee effect and found periodic fishing to yield higher economic benefits for fish populations. Liu et al. [24] studied the dynamic behavior of the Leslie Power model with weak Allee effect and fear effect. However, there is limited research on the effects of different Allee effects on fisheries economic models. Therefore, it is necessary for this article to consider the impact of different Allee effects on system dynamics.

Fast-slow systems have been widely applied in fields such as physics, chemistry, pharmacology, and ecology. A key feature of these systems is that their different variables vary over two or more time scales and such systems are typically handled by geometric singular perturbation theory [9]. In ecosystems, considering the difference in growth rates between prey and predators, the relationship between the two can be established using a fast-slow system [6, 21, 32]. Saha et al. [31] investigated a predator-prey model with Beddington–DeAngelis response, revealed rich dynamics including relaxation oscillations, canard cycles, and canard explosions. Li and Zhang [22] discussed the dynamic behavior of a fast-slow Leslie–Gower predator-prey model with constant harvesting. As mentioned in reference [3], there is a significant disparity between the rate of change in fishing effort and that in fish species. Therefore, the fast-slow system is also applicable to the fishery economic model, and discussing the fast-slow dynamics of the fishery economic model is also very interesting.

In the natural environment, the number and structure of biological populations are affected by a variety of random factors, such as climate change and random fluctuations in food resources. Stochastic differential equations are frequently employed to simulate random fluctuations in biological systems, as a result, they play an important role in studying the dynamic analysis of systems [14,26,29,42]. Yu [41] proposed and explored a single species model with Allee effect driven by correlated colored noise. Wang [36] studied a population model with Allee effect affected by both additive and multiplicative noise, and the results showed that correlated noise has a complex impact on the final population size distribution. Han and Jiang [12] considered and studied a stochastic predator-prey system with general infinite delay, and provided the necessary conditions for species persistence and extinction. Overall, environmental noise has a complex impact on the final distribution of population size.

Based on the above analysis, although some scholars have proposed that there is a significant difference between the rate of change in capture effort and the growth rate of species, few have specifically discussed the fast-slow dynamic properties of fast-slow fishery economic models. Therefore, we consider the Allee effect in fish populations and the influence of external factors on both fish populations and catches, and establish a stochastic fast-slow fishery economic model. We use singular perturbation techniques to study the complex fast-slow dynamics of the model and discuss the bifurcation behavior of the random fast-slow system. The structure of this article is as follows: In Section 2, a fast-slow fishery economic model with Allee effect is proposed, and the existence of equilibrium is discussed. In Section 3, we discuss the bifurcation behavior of deterministic system, which can generate transcritical bifurcation and Hopf bifurcation. In Section 4, we use singular perturbation theory to discuss the singular Hopf bifurcation and relaxation oscillation generated by fast-slow system, and investigate the existence of stationary distributions for stochastic fast-slow reduction system. In Section 5, we consider the time scale parameter ε as a general parameter and discuss the existence of stationary distribution for stochastic systems with weak Allee effects, as well as the dynamic behavior generated by the stochastic system. In Section 6, the conclusion and outlook are elaborated.

2 Model establishment and equilibrium analysis

2.1 Model establishment

In this section, we consider a single population fishery economic model, which takes the following form:

$$\begin{cases} \dfrac{dx}{dt} = rx\left(1-\dfrac{x}{K}\right)(x-A) - qEx, \\ \dfrac{dE}{dt} = m\,(pqx-c)\,E, \end{cases} \tag{2.1}$$

where the growth of the fish population follows logistic growth, x represents the density of the fish population at time t, E represents the effort required for capture, which is positively correlated with the total profit. Table 2.1. provides the biological explanations for the parameters in the model.

Parameter	Biological Interpretation
r	Intrinsic growth rate of fish stocks
K	Maximum environmental capacity of fish stocks
A	Allee effect threshold, where $0 < A < K$ indicates strong Allee effect, and $-K < A < 0$ indicates weak Allee effect
m	Adjustment coefficient of E
p	The price per unit of catch of fish stocks
q	Capture coefficient
c	Unit fishing cost of fish stocks

Table 2.1: Definition of Parameters in system (2.1)

Perform a dimensionless transformation on system (2.1),

$$x \to \frac{x}{K}, \quad t \to rt,$$

we have

$$\begin{cases} \dfrac{dx}{dt} = x\,(1-x)\,(Kx-A) - \alpha E x & =: f(x,E,\varepsilon), \\ \dfrac{dE}{dt} = \varepsilon\,(\beta p x - c)\,E & =: \varepsilon g(x,E,\varepsilon), \end{cases} \tag{2.2}$$

where new dimensionless parameters are $\alpha = \frac{q}{r}$, $\beta = qK$, $\varepsilon = \frac{m}{r}$. These parameters are positive. Since m is an adjustment parameter for E, which is a very small number, there is $m \ll r$, resulting in $0 < \varepsilon \ll 1$. At this point, system (2.2) is a fast-slow fishery economic system.

Let $\tau = \varepsilon t$, the system (2.2) becomes that

$$\begin{cases} \varepsilon\dfrac{dx}{d\tau} = x\,(1-x)\,(Kx-A) - \alpha E x & =: f(x,E,\varepsilon), \\ \dfrac{dE}{d\tau} = (\beta p x - c)\,E & =: g(x,E,\varepsilon). \end{cases} \tag{2.3}$$

Under nonnegative initial conditions, the dynamics of the system will be limited within the first quadrant. We name t as the fast time scale and τ as the slow time scale. When $0 < \varepsilon \ll 1$, x evolves on a fast time scale t and E evolves on a slow time scale τ. Therefore, we refer to x as a fast variable and E as a slow variable.

2.2 Equilibrium analysis

In the section, the existence of equilibrium points and the stability of certain equilibrium points within system (2.2) will be discussed. From a biological perspective, we only focus on the dynamic behavior of system (2.2) in region $\mathbb{R}^2_+ = \{(x,E) : x \geq 0, E \geq 0\}$.

There are three boundary equilibrium points $S_1(0,0)$, $S_2(1,0)$ and $S_3(\frac{A}{K},0)$ in system (2.2). There exists a unique internal equilibrium point $S_*\,(x_*,E_*)$ if $\frac{A}{K} < \frac{c}{\beta p} < 1$, where $x_* = \frac{c}{\beta p}$, $E_* = \frac{(1-x_*)(Kx_*-A)}{\alpha}$.

The Jacobian matrix of system (2.2) at (x,E) is

$$J := \begin{pmatrix} -3Kx^2 + 2(K+A)x - A - \alpha E & -\alpha E \\ \varepsilon\beta p E & \varepsilon(\beta p x - c) \end{pmatrix}.$$

The Jacobian matrix at $S_1(0,0)$ is

$$J|_{S_1} = \begin{pmatrix} -A & 0 \\ 0 & -c\varepsilon \end{pmatrix},$$

and its corresponding eigenvalues are $\lambda_1 = -A$ and $\lambda_2 = -c\varepsilon$, where λ_1 is influenced by the Allee effect type. Therefore, under the strong Allee effect $0 < A < K$, S_1 is a stable node, and under the weak Allee effect $A < 0$, S_1 is an unstable node.

The Jacobian matrix at $S_2(1,0)$ is

$$J|_{S_2} = \begin{pmatrix} A-K & -\alpha \\ 0 & \varepsilon(\beta p - c) \end{pmatrix},$$

and its corresponding eigenvalues are $\lambda_1 = A - K$ and $\lambda_2 = \varepsilon(\beta p - c)$. The stability of equilibrium point S_2 is not affected by the Allee effect. When $c > \beta p$, S_2 is stable node, and when $c < \beta p$, S_2 is unstable node.

The Jacobian matrix at $S_3(\frac{A}{K}, 0)$ is

$$J|_{S_3} = \begin{pmatrix} A\left(1 - \dfrac{A}{K}\right) & -\frac{A\alpha}{K} \\ 0 & \varepsilon\left(\dfrac{\beta p A}{K} - c\right) \end{pmatrix},$$

and its corresponding eigenvalues are $\lambda_1 = A(1 - \frac{A}{K})$ and $\lambda_2 = \varepsilon(\frac{\beta p A}{K} - c)$. Under the strong Allee effect $0 < A < K$, $\lambda_1 < 0$, so S_3 is a saddle point for $c > \frac{\beta p A}{K}$ and S_3 is an unstable node for $c < \frac{\beta p A}{K}$. Under the weak Allee effect $A < 0$, S_3 is a non positive equilibrium point, we will not discuss it.

The Jacobian matrix at $S_*(x_*, E_*)$ (whose existence condition is $\frac{A}{K} < \frac{c}{\beta p} < 1$) is

$$J|_{S_*} = \begin{pmatrix} \dfrac{c}{\beta p}\left(A + K - \dfrac{2Kc}{\beta p}\right) & -\dfrac{\alpha c}{\beta p} \\ \dfrac{\varepsilon \beta p}{\alpha}\left(1 - \dfrac{c}{\beta p}\right)\left(\dfrac{Kc}{\beta p} - A\right) & 0 \end{pmatrix}.$$

The corresponding characteristic equation is

$$|\lambda E - J|_{S_*} = \lambda^2 + q_1\lambda + q_2 = 0, \tag{2.4}$$

where $q_1 = -\frac{c}{\beta p}(A + K - \frac{2Kc}{\beta p})$, $q_2 = c\varepsilon(1 - \frac{c}{\beta p})(\frac{Kc}{\beta p} - A)$. Since $\frac{A}{K} < \frac{c}{\beta p} < 1$, we can obtain $q_2 > 0$. By using the Veda theorem, we can conclude that if $q_1 = 0$ i.e. $c = \frac{(A+K)\beta p}{2K}$, its eigenvalues are a pair of pure imaginary roots, so S_* is a center; if $q_1 > 0$, the real parts of its eigenvalues are all negative, so S_* is locally asymptotically stable; and if $q_1 < 0$, the real parts of its eigenvalues are all positive, S_* is unstable.

3 Bifurcation analysis

In this section, we mainly discuss the dynamic behavior of the system (2.2). We delve into the bifurcation behavior of the system (2.2) at the boundary equilibrium and analyze the existence and stability of its Hopf bifurcation at the internal equilibrium $S_*(x_*, E_*)$.

3.1 Transcritical bifurcation

Theorem 3.1. *For system (2.2), a transcritical bifurcation will occur near the equilibrium point S_2 as the bifurcation parameter c passes through $c^* = \beta p$.*

Proof. We know that S_2 is stable with $c > \beta p$ and S_2 is unstable with $c < \beta p$. That is, as the value of parameter c passes through βp, the stability of S_2 changes, so there may be a transcritical bifurcation. Next, we prove the bifurcation behavior at equilibrium point S_2 by using Sotomayor's theorem to .

Denote

$$X = (x, E)^{\mathrm{T}},\ F(X, c) = \begin{pmatrix} x(1-x)(Kx - A) - \alpha E x \\ \varepsilon(\beta p x - c)E \end{pmatrix},$$

$J|_{S_2} = DF(S_2, \beta p)$ has a zero eigenvalue at $c^* = \beta p$, and its corresponding eigenvector is $\vartheta = (\alpha, A-K)^{\mathrm{T}} = (\vartheta_1, \vartheta_2)^{\mathrm{T}}$. The eigenvector corresponding to the zero eigenvalue of transpose matrix $D^{\mathrm{T}}F(S_2, \beta p)$ is $\omega = (0,1)^{\mathrm{T}}$. After calculation, it is easy to obtain the following formula:

$$\begin{aligned} F_c(S_2, \beta p) &= \begin{pmatrix} 0 \\ 0 \end{pmatrix}, \\ DF_c(S_2, \beta p)\vartheta &= \begin{pmatrix} 0 \\ \varepsilon(K-A) \end{pmatrix}, \\ D^2F_c(S_2, \beta p)(\vartheta, \vartheta) &= \begin{pmatrix} \alpha^2(A-3K) \\ \varepsilon\beta p\alpha(A-K) \end{pmatrix}. \end{aligned}$$

Furthermore, it can be obtained that

$$\begin{aligned} \omega^{\mathrm{T}} F_c(S_2, \beta p) &= 0, \\ \omega^{\mathrm{T}}[DF_c(S_2, \beta p)\vartheta] &= \varepsilon(K-A) \neq 0, \\ \omega^{\mathrm{T}}[D^2F_c(S_2, \beta p)(\vartheta, \vartheta)] &= \varepsilon\beta p\alpha(A-K) \neq 0. \end{aligned}$$

Therefore, according to Sotomayor's theorem, system (2.2) undergoes a transcritical bifurcation at equilibrium point S_2 if $c^* = \beta p$. □

3.2 Hopf bifurcation

In two-dimensional systems, singular Hopf bifurcation is a special case of Hopf bifurcation, therefore, it is necessary to discuss the existence and stability of Hopf bifurcation.

According to the analysis in Subsection 2.2, we know that S_* is a center if $c = \frac{(A+K)\beta p}{2K}$, and the stability of S_* changes as the c value passes through $\frac{(A+K)\beta p}{2K}$. Therefore, Hopf bifurcation may occur at this equilibrium point.

Lemma 3.2. *System (2.2) will generate supercritical Hopf bifurcation near the equilibrium point $S_*(x_*, y_*)$, as the bifurcation parameter c passes through $\tilde{c} = \frac{(A+K)\beta p}{2K}$.*

Proof. Select c as the bifurcation parameter, with a bifurcation parameter threshold $\tilde{c} = \frac{(A+K)\beta p}{2K}$ that satisfies $\det(J|_{S_*}) > 0$ and $\mathrm{tr}(J|_{S_*}) = 0$. When $c = \tilde{c} = \frac{(A+K)\beta p}{2K}$, equation (2.4) has a pair of pure imaginary roots $\pm\sqrt{q_2}$, where $q_2 = c\varepsilon(1 - \frac{c}{\beta p})(\frac{Kc}{\beta p} - A)$. Next, we will verify the transversality condition for Hopf bifurcation. Assuming that $\lambda = \varphi(c) + i\psi(c)$ a root of the characteristic equation (2.4), we can obtain that $\varphi(\tilde{c}) = 0$, $\psi(\tilde{c}) = \sqrt{q_2}$. Substituting $\lambda = \varphi(c) + i\psi(c)$ into equation (2.4) and separating the real and imaginary parts, we obtain

$$\begin{cases} \varphi^2 - \psi^2 + q_1\varphi + q_2 = 0, \\ 2\varphi\psi + q_1\psi = 0. \end{cases}$$

After taking the derivative of c at both ends of the above equation, we obtain

$$\begin{cases} -2\psi\psi' + q_1\varphi' + q_2' = 0, \\ 2\varphi' + q_1' = 0. \end{cases}$$

After further calculation, we obtain $\frac{d\varphi}{dc}|_{c=\tilde{c}} = -\frac{A+K}{2\beta p} \neq 0$, which satisfies the transversality condition for Hopf bifurcation. Next, we will discuss the stability of Hopf bifurcation, it can help determine under what conditions ecosystems can maintain equilibrium. We take the transformation $\bar{x} = x - x_*$, $\bar{E} = E - E_*$ to move (x_*, E_*) to the origin. Then dropping the bars, the system (2.2) performs Taylor expansion at the origin, and we obtain:

$$\begin{cases} \frac{dx}{dt} = a_{10}x + a_{01}E + a_{20}x^2 + a_{11}xE + a_{02}E^2 \\ \qquad + a_{30}x^3 + a_{21}x^2E + a_{12}xE^2 + a_{03}E^3 + o(|x,E|^4), \\ \frac{dE}{dt} = b_{10}x + b_{01}E + b_{20}x^2 + b_{11}xE + b_{02}E^2 \\ \qquad + b_{30}x^3 + b_{21}x^2E + b_{12}xE^2 + b_{03}E^3 + o(|x,E|^4), \end{cases} \tag{3.1}$$

where

$$a_{10} = x_*(A + K - 2Kx_*), \quad a_{01} = -\alpha x_*, \quad a_{20} = -3Kx_* + A + K,$$
$$a_{11} = -\alpha, \quad a_{30} = -K, \quad b_{10} = \frac{\varepsilon\beta p}{\alpha}(1 - x_*)(Kx_* - A), \quad b_{11} = \varepsilon\beta p,$$
$$a_{02} = a_{21} = a_{12} = a_{03} = b_{01} = b_{20} = b_{02} = b_{30} = b_{21} = b_{12} = b_{03} = 0.$$

The Jacobian matrix of system (3.1) at $(0,0)$ is

$$J|_{(0,0)} = \begin{pmatrix} x_*(A + K - 2Kx_*) & -\alpha x_* \\ \frac{\varepsilon\beta p}{\alpha}(1 - x_*)(Kx_* - A) & 0 \end{pmatrix}.$$

Through simple calculations, we can obtain $\mathrm{tr}(J|_{(0,0)}) = 0$ and $\det(J|_{(0,0)}) = \varepsilon\beta p x_*(1 - x_*)(Kx_* - A) > 0$ at $c = \tilde{c}$. Thus, $J|_{(0,0)}$ has a pair of pure imaginary eigenvalue

$$\lambda = \pm i\sqrt{\varepsilon\beta p x_*(1 - x_*)(Kx_* - A)} \quad \text{for } c = \tilde{c}.$$

Furthermore, the first Lyapunov coefficient l_1 [30] for determining the stability of the limit cycle is given:

$$l_1 = -\frac{3\pi}{2a_{01}D^{\frac{3}{2}}}\sum_{i=1}^{8}\xi_i,$$

where

$$D = a_{10}b_{01} - a_{01}b_{10}, \quad \xi_1 = \varepsilon\alpha\beta p x_*(1 - x_*)(Kx_* - A)(A + K - 2Kx_*),$$
$$\xi_2 = -\varepsilon\alpha\beta p x_*^2(A + K - 2Kx_*)(\varepsilon\beta p - 3Kx_* + A + K), \quad \xi_3 = \xi_4 = 0,$$
$$\xi_5 = 2\alpha x_*^2(A + K - 2Kx_*)(A + K - 3Kx_*)^2, \quad \xi_6 = 0,$$
$$\xi_7 = \left(\varepsilon\alpha\beta p x_*(1 - x_*)(Kx_* - A) + 2\alpha x_*^2(A + K - 2Kx_*)^2\right)(3Kx_* - A - K),$$
$$\xi_8 = 3\alpha K x_*^3(A + K - 2Kx_*)^2 - 3\varepsilon\alpha\beta p K x_*^2(1 - x_*)(Kx_* - A).$$

After substituting $x_* = \frac{c}{\beta p}$ and $\tilde{c} = \frac{(A+K)\beta p}{2K}$ into the calculation, and since $|A| < K$, we obtain

$$\begin{aligned} l_1 &= \left(\frac{3\pi K}{\alpha(A+K)\left(\frac{1}{2}\right)^{\frac{3}{2}}\left(\frac{\varepsilon\beta p A^3}{4K^2} - \frac{p\beta\varepsilon A^2}{4K} - \frac{A\beta p\varepsilon}{4} + \frac{K\beta p\varepsilon}{4}\right)^{\frac{3}{2}}}\right)\left(-\frac{K^2\alpha\beta p\varepsilon}{8} - \frac{A^4\alpha\beta p\varepsilon}{8K^2} + \frac{A^2\alpha\beta p\varepsilon}{4}\right) \\ &= -\left(\frac{3\pi K}{\alpha(A+K)\left(\frac{1}{2}\right)^{\frac{3}{2}}\left(\frac{\varepsilon\beta p}{4K^2}(K-A)^2(K+A)\right)^{\frac{3}{2}}}\right)\frac{\alpha\beta p\varepsilon}{8K^2}(K^2 - A^2)^2 \\ &= -\frac{6\sqrt{2}\pi K^2}{(K-A)\sqrt{\varepsilon\beta p(K+A)}} < 0. \end{aligned}$$

Therefore, system (2.2) generates a supercritical Hopf bifurcation near the equilibrium point $S_*(x_*, E_*)$. □

3.3 Numerical simulation

In this section, we verify the conclusions given earlier through numerical simulations. For system (2.2) with strong Allee effect, we select parameter $K = 3$, $A = 0.8$, $\alpha = 0.17$, $\varepsilon = 0.5$, $\beta = 1.5$, $p = 3$ (The data source from Table 3.2.).

Parameter	Reference range	Data sources
r	$[0.3, 0.9]$	[4,28]
K	$[2, 10]$	[33]
A	$[-1, 0) \cup (0, 1]$	[38,43]
m	$[0.01, 0.4]$	[10]
p	$[3, 15]$	[5]
q	$[0.1, 1.5]$	[5,39]
c	$[1, 15]$	[5]

Table 3.1: Parameter selection range in Model (2.1).

Parameter	Reference range
K	$[2, 10]$
A	$[-1, 0) \cup (0, 1]$
$\alpha = \frac{q}{r}$	$[0.1, 1.5]$
$\beta = qK$	$[0.2, 15]$
p	$[3, 15]$
c	$[1, 15]$
$\varepsilon = \frac{m}{r}$	[0.01,1.3]

Table 3.2: Range of parameter values in system (2.2).

After calculation, it can be concluded that the bifurcation parameter value $c_H = 2.85$, and $S_*(x_*, E_*) = (0.6311, 2.3725)$. According to Lemma 3.2, it is known that a supercritical Hopf bifurcation will occur. As shown in Figure 3.1(a). Figure 3.1(b) is a time series graph of x and E. Figure 3.1(c) is the phase diagram of system (2.2). Furthermore, selecting parameter $\varepsilon = 0.5$, $c = 2.89 > c_H$, we can obtain that the equilibrium point S_* is locally asymptotically stable. (See Fig. 3.2).

For system (2.2) with weak Allee effect, we select parameter $K = 3$, $A = -0.3$, $\alpha = 0.17$, $\varepsilon = 0.5$, $\beta = 1.5$, $p = 3$ (the data source from Table 3.2.). After calculation, it can be concluded that the bifurcation parameter value $c_H = 2.025$, and $S_*(x_*, E_*) = (0.4444, 5.3377)$. As shown in Figure 3.1(d-f).

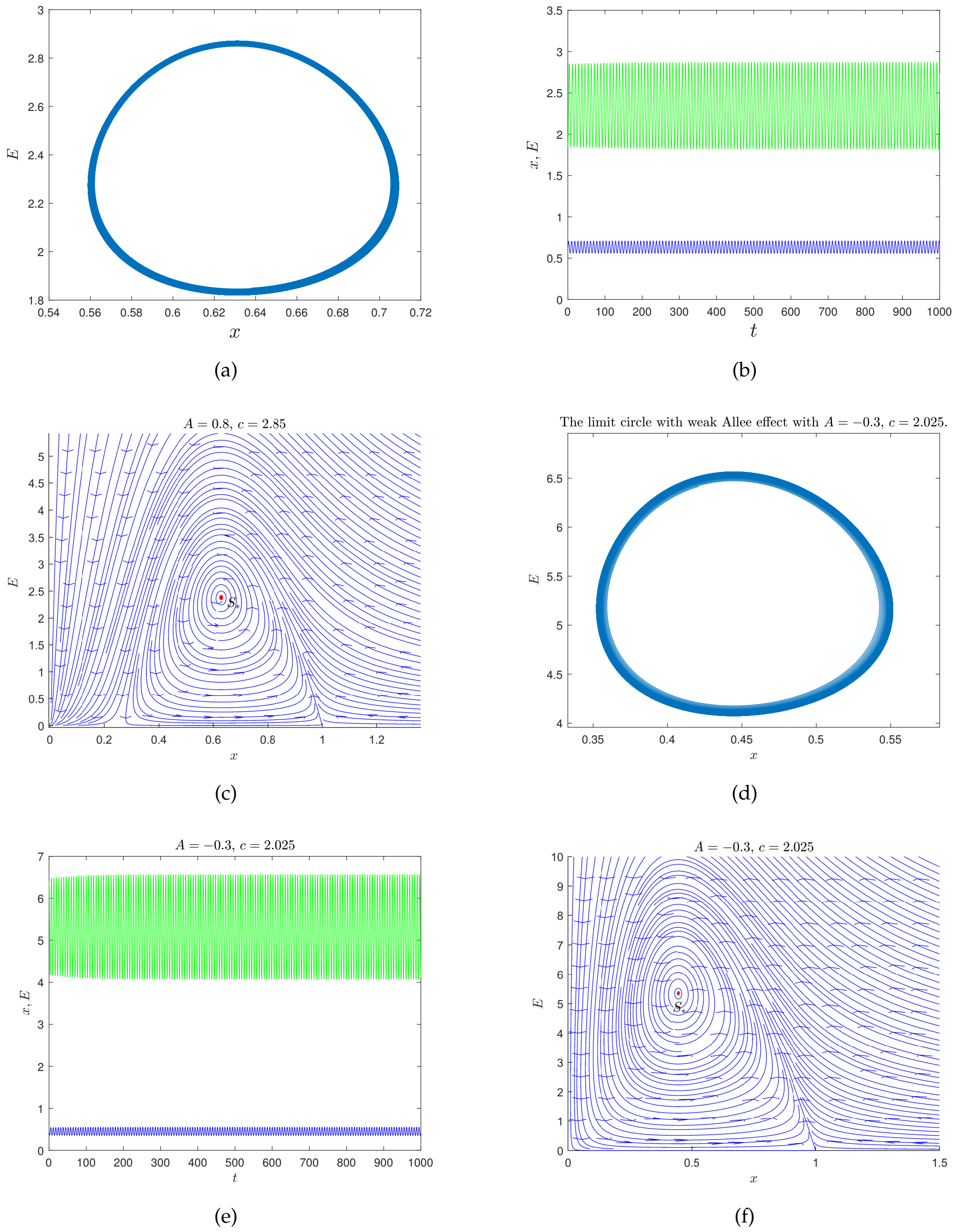

Figure 3.1: Phase plane analysis of system (2.2). (a, d) The periodic cyclic orbit generated by the system (2.2). (b, d) $x - t$ (blue) and $E - t$ (green) time series diagram. (c, f) The phase diagram of system (2.2).

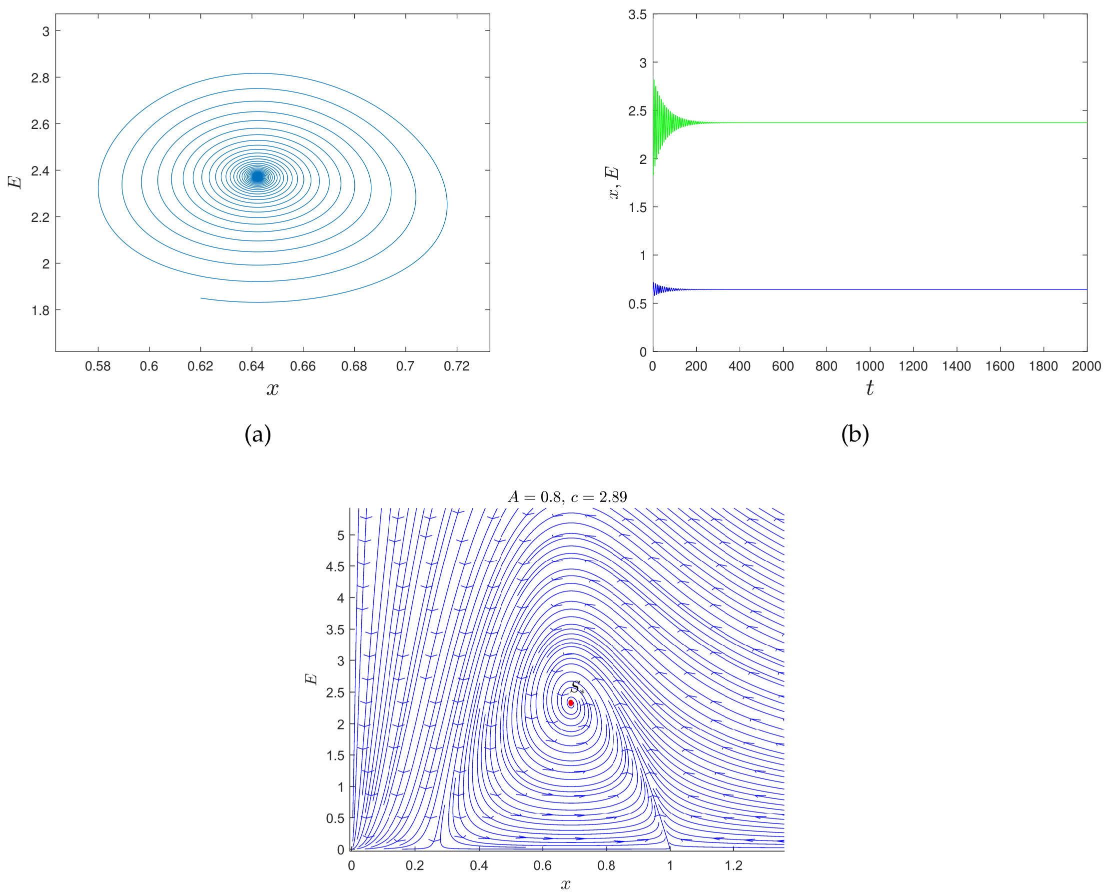

(c)

Figure 3.2: Phase plane analysis of system (2.2) for $A = 0.8$ and $c = 2.89$. (a) The equilibrium point S_* is locally asymptotically stable when $K = 3$, $A = 0.8$, $\alpha = 0.17$, $\varepsilon = 0.5$, $\beta = 1.5$, $p = 3$, $c = 2.89$. (b) $x - t$ (blue) and $E - t$ (green) time series diagram. (c) The phase diagram of system (2.2).

4 Singular perturbation analysis

In this section, we use singular perturbation theory [9] to discuss the fast-slow dynamic behavior of system (2.2). Under the strong Allee effect, system (2.2) will generate a singular Hopf bifurcation near the internal equilibrium point. Under the weak Allee effect, the dynamical behavior generated by system (2.2) is more complex, resulting not only in singular Hopf bifurcations but also relaxation oscillations.

4.1 Asymptotic expansion of critical manifolds

Let $\varepsilon \to 0$, system (2.2) becomes

$$\begin{cases} \dfrac{dx}{dt} = f(x, E, 0), \\ \dfrac{dE}{dt} = 0, \end{cases} \tag{4.1}$$

which is called the fast subsystem or layer equation, and the corresponding flow is called fast flow. Let $\varepsilon \to 0$, system (2.3) can be reduced to a differential algebraic system given by

$$\begin{cases} 0 = f(x, E, 0), \\ \dfrac{dE}{d\tau} = g(x, E, 0), \end{cases} \tag{4.2}$$

which is called the slow subsystem, and the flow it generates is called slow flow. The slow flow is constrained in set $C_0 = \{(x, E) \in \mathbb{R}_+^2, f(x, E, \varepsilon) = 0\}$. C_0 is called the critical manifold, which consists of two parts and is given by

$$\begin{aligned} C_0 = C_{10} \cup C_{20} &= \left\{(x, E) \in \mathbb{R}_+^2,\ x = 0\right\} \\ &\cup \left\{(x, E) \in \mathbb{R}_+^2,\ E = u_0(x),\ u_0(x) = \frac{(1-x)(Kx-A)}{\alpha},\ \frac{A}{K} < x < 1,\ E > 0\right\}, \end{aligned} \tag{4.3}$$

which is the critical manifold of system (2.2) with strong Allee effect($0 < A < K$). The critical manifold C_{20} is similar to a parabola, with its maximum value being the fold point $P(x_f, E_f)$, where $x_f = \frac{A+K}{2K}$ and $E_f = \frac{(1-x_f)(Kx_f-A)}{\alpha}$. The nonhyperbolic fold point divides the critical manifold C_0 into two parts: the attracting sub-manifold $C_0^a = C_{20}^a \cup C_{10} = \{(x, E) \in \mathbb{R}_+^2,\ x_f < x < 1\} \cup C_{10}$ and the repelling sub-manifold $C_0^r = C_{20}^r = \{(x, E) \in \mathbb{R}_+^2,\ \frac{A}{K} < x < 1\}$ (see Figure 4.1(a)).

For weak Allee effect ($A < 0$), the slow flow generated by the slow subsystem is limited to the critical manifold

$$\begin{aligned} C_0 = C_{10} \cup C_{20} &= \left\{(x, E) \in \mathbb{R}_+^2,\ x = 0\right\} \\ &\cup \left\{(x, E) \in \mathbb{R}_+^2,\ E = u_0(x),\ u_0(x) = \frac{(1-x)(Kx-A)}{\alpha}, 0 < x < 1,\ E > 0\right\}. \end{aligned} \tag{4.4}$$

After calculation, we obtain a maximum point $P(x_f, E_f)$, where $x_f = \frac{A+K}{2K}$, $E_f = \frac{(1-x_f)(Kx_f-A)}{\alpha}$, a transcritical point $B(0, E_B) = (0, -\frac{A}{\alpha})$, and a boundary point $C(x_C, 0) = (1, 0)$. The critical manifold C_0 can be partitioned into two segments:

$$C_0^a = C_{10}^a \cup C_{20}^a = \left\{(x, E) \in \mathbb{R}_+^2, x = 0, E > -\frac{A}{\alpha}\right\} \cup \left\{(x, E) \in \mathbb{R}_+^2, x_f < x < 1\right\},$$

$$C_0^r = C_{10}^r \cup C_{20}^r = \left\{(x, E) \in \mathbb{R}_+^2, x = 0, 0 < E < -\frac{A}{\alpha}\right\} \cup \left\{(x, E) \in \mathbb{R}_+^2, 0 < x < x_f\right\},$$

where C_0^a is normally attracting and C_0^r is normally repelling (see Figure 4.1(b)). According to the Fenichel's Theorem [19], there exists a locally invariant manifold C_ε with differential homeomorphism at C_{20}. The Hausdorff distance from C_ε to C_{20} is $O(\varepsilon)$, and the flow on C_ε converges to a slow flow when ε tends to 0. Therefore, C_ε can be seen as a small perturbation of C_{20}, given by:

$$C_\varepsilon := u_0(x) + \varepsilon u_1(x) + \varepsilon^2 u_2(x) + \cdots = C_{20} + O(\varepsilon), \tag{4.5}$$

where $u_0(x)$ is the critical manifold of C_{20} as given by (4.3). In addition, we use C_ε^a and C_ε^r represent the perturbed attracting sub-manifold and repelling sub-manifold, respectively. Due to the local invariance of approximating manifold C_ε, we have

$$\frac{dE}{dt} = \frac{dE}{dx}\frac{dx}{dt} = \left(\frac{du_0}{dx} + \varepsilon\frac{du_1}{dx} + \varepsilon^2\frac{du_2}{dx} + \dots\right)\frac{dx}{dt}. \tag{4.6}$$

Substituting $\frac{dE}{dt}$ and $\frac{dx}{dt}$ into equation (4.6), and by comparing the coefficients of ε, it can be

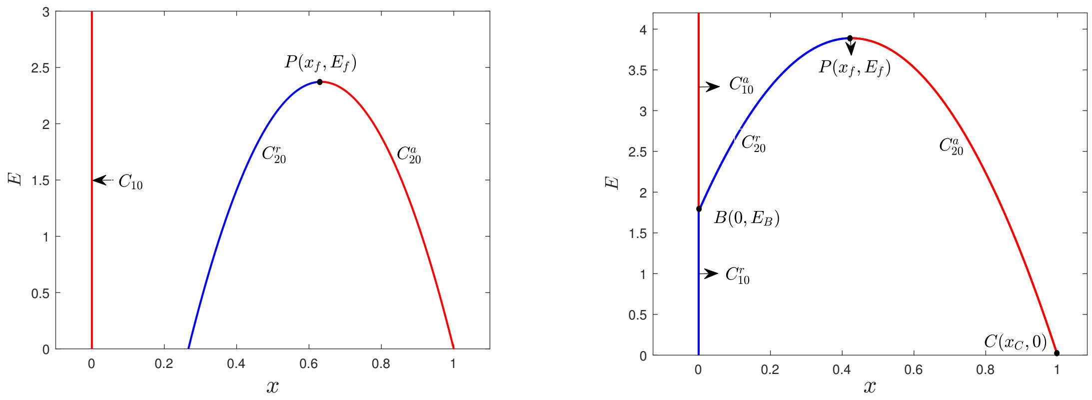

(a) (b)

Figure 4.1: The critical manifold. (a) The critical manifold of system (2.2) with strong Allee effect. (b) The critical manifold of system (2.2) with weak Allee effect. The blue lines represent the repelling sub-manifold of the critical manifold, and the red lines represent the attracting sub-manifold of the critical manifold.

obtained that

$$u_1(x) = \frac{(c - \beta p x) u_0}{\alpha x \frac{du_0}{dx}}.$$

By comparing the coefficients of ε^2, it can be concluded that

$$u_2(x) = \frac{(c - \beta p x - \alpha x \frac{du_1}{dx}) u_1}{\alpha x \frac{du_1}{dx}}.$$

Using the same method, $u_j(x), j = 3, 4, \ldots$ can be obtained. But according to Fenichel's theorem, perturbation manifolds cannot be extended at fold points (x_f, E_f) that lose hyperbolic properties [6].

4.2 Singular Hopf bifurcation

In this section, we discuss the existence of singular Hopf bifurcation of system (2.2). And we do not limit the threshold of the Allee effect, that is, whether it is strong or weak Allee effect, system (2.2) will produce singular Hopf bifurcation.

According to the analysis in Subsection 2.2, the system has an internal equilibrium point (x_*, E_*) for $\frac{A}{K} < \frac{c}{\beta p} < 1$. The Jacobian matrix at this point is

$$J|_{S_*}^t = \begin{pmatrix} \frac{c}{\beta p}\left(A + K - \frac{2Kc}{\beta p}\right) & -\frac{\alpha c}{\beta p} \\ \frac{\varepsilon \beta p}{\alpha}\left(1 - \frac{c}{\beta p}\right)\left(\frac{Kc}{\beta p} - A\right) & 0 \end{pmatrix},$$

where t represents the Jacobian matrix of the system at S_* at a fast time scale.

According to the Hopf bifurcation principle, we need to solve the Hopf bifurcation threshold to satisfy that the trace of $J|_{S_*}^t$ is equal to 0 and the determinant value of $J|_{S_*}^t$ is greater than 0, which means that $q_1 = 0$ and $q_2 > 0$ in (2.4). Taking c as the bifurcation parameter, we obtain the bifurcation threshold

$$c_H = \frac{(A+K)\beta p}{2K},$$

and the equilibrium (x_H, E_H) at $c = c_H$, where $x_H = \frac{c}{\beta p}$, $E_H = \frac{(1-x_*)(Kx_*-A)}{\alpha}$. This point coincides perfectly with the fold point. At the Hopf bifurcation threshold, $J|_{S_*}^{t}$ has a pair of pure imaginary eigenvalues:

$$\lambda_H(\sqrt{\varepsilon}) = \pm i\sqrt{\frac{(K-A)^2(A+K)\beta p\varepsilon}{8K^2}}.$$

Theorem 4.1. *Set* $0 < \varepsilon \ll 1$. *Assuming* (x_f, E_f) *is the generic folded singularity of system* (2.2), *system* (2.2) *undergoes a singular Hopf bifurcation in a certain domain of* x_f *when* $c = c_H$, *resulting in a stable canard cycles. In addition, there exists a singular Hopf bifurcation curve* $\delta = \delta_H(\sqrt{\varepsilon})$ *such that* (x_f, E_f) *is stable when* $\delta < \delta_H(\sqrt{\varepsilon})$ *and*

$$\delta_H(\sqrt{\varepsilon}) = -\frac{a_1 + a_5}{2}\varepsilon + \mathcal{O}(\varepsilon^{\frac{3}{2}}). \tag{4.7}$$

Proof. First, we discuss that (x_f, E_f) is a generic folded singularity. By calculation, it can be concluded that (x_f, E_f) satisfies the following conditions:

$$\begin{aligned} f(x_f, E_f) &= 0, & f_x(x_f, E_f) &= 0, \\ f_{xx}(x_f, E_f) &\neq 0, & f_y(x_f, E_f) &\neq 0, \end{aligned}$$

and

$$g(x_f, E_f) = 0,$$

thus (x_f, E_f) is a fold singularity. In addition, it satisfies the condition:

$$g_x(x_f, E_f) \neq 0, \quad g_c(x_f, E_f) \neq 0,$$

thus (x_f, E_f) is a generic fold singularity.

In order to study the local behavior of system (2.2) near $P(x_f, E_f)$, we perform coordinate transformation

$$u = x - x_*, \quad v = E - E_*, \quad \delta = c - c_H,$$

and system (2.2) becomes

$$\begin{cases} \dfrac{du}{dt} = -vh_1(u,v,\delta,\varepsilon) + u^2h_2(u,v,\delta,\varepsilon) + \varepsilon h_3(u,v,\delta,\varepsilon), \\ \dfrac{dv}{dt} = \varepsilon\left\{uh_4(u,v,\delta,\varepsilon) - \delta h_5(u,v,\delta,\varepsilon) + vh_6(u,v,\delta,\varepsilon) + o(|u,v,\delta|^3)\right\}, \end{cases} \tag{4.8}$$

where

$$\begin{aligned} h_1(u,v,\delta,\varepsilon) &= \alpha u + \alpha x_*, \\ h_2(u,v,\delta,\varepsilon) &= A + K - 3Kx_* - Ku, \\ h_3(u,v,\delta,\varepsilon) &= 0, \\ h_4(u,v,\delta,\varepsilon) &= \beta p v + \beta p E_*, \\ h_5(u,v,\delta,\varepsilon) &= v + E_*, \\ h_6(u,v,\delta,\varepsilon) &= \beta p x_* - c_H. \end{aligned}$$

According to the theory in [19], we have obtained

$$
\begin{aligned}
a_1 &= \frac{\partial h_3}{\partial u}(0,0,0,0) = 0,\\
a_2 &= \frac{\partial h_1}{\partial u}(0,0,0,0) = \alpha,\\
a_3 &= \frac{\partial h_2}{\partial u}(0,0,0,0) = -K,\\
a_4 &= \frac{\partial h_4}{\partial u}(0,0,0,0) = 0,\\
a_5 &= h_6(0,0,0,0) = \beta p x_* - c_H.
\end{aligned} \tag{4.9}
$$

After further calculation, the Hopf bifurcation curve is obtained to be

$$\delta_H(\sqrt{\varepsilon}) = -\frac{a_1 + a_5}{2}\varepsilon + \mathcal{O}(\varepsilon^{\frac{3}{2}}) = \mathcal{O}(\varepsilon^{\frac{3}{2}}),$$

and the maximum canard curve is

$$\delta_c(\sqrt{\varepsilon}) = -\Big(\frac{a_1 + a_2}{2} + \frac{A}{8}\Big)\varepsilon + \mathcal{O}(\varepsilon^{\frac{3}{2}}) = \frac{\alpha + 3K}{8} + \mathcal{O}(\varepsilon^{\frac{3}{2}}). \qquad \square$$

Compared with the Hopf bifurcation in Subsection 3.1, we can find that the singular Hopf bifurcation coincides exactly with the case of the aforementioned Hopf bifurcation. Thus, the stability of periodic solutions generated by singular Hopf bifurcation is the same as that of Hopf bifurcation. According to Lemma 3.2, system (2.2) undergoes a supercritical singular Hopf bifurcation for $l_1 < 0$. According to [19], we can calculate that system (2.2) will generate a singular supercritical Hopf bifurcation by calculating $A_1 = -a_2 + 3a_3 - 2a_4 + 2a_5 = -\alpha - 3K < 0$. The conclusion obtained from Lemma 3.2 is also consistent.

Through numerical simulation, we verify the above conclusion. A canard without head will be generated, when $K = 3$, $A = 0.8$, $\alpha = 0.17$, $\varepsilon = 0.05$, $\beta = 1.5$, $p = 3$, $c = 2.8446$, (see Figure 4.2). Compared with Hopf bifurcation, under the influence of perturbation parameter ε, the bottom of the limit cycle generated by the singular Hopf bifurcation will be flatter. By comparing Figure 3.1(a) with Figure 4.2(a), it can be seen.

Remark 4.2. Fishing effort refers to the amount of work invested in a fishery using the same fishing operation method over a period of time, reflecting the mortality level of the captured resource population. The emergence of Hopf bifurcation and singular Hopf bifurcation indicates that the system will experience periodic fluctuations, which means that population density and capture effort will show periodic changes. This also means that there is a dynamic balance between population density and mortality rate, and the ecosystem is in a state of dynamic equilibrium.

4.3 Relaxation oscillation

Compared with system (2.2) with strong Allee effect, system (2.2) with weak Allee effect produce more complex dynamical behavior, resulting to relaxation oscillations. This section mainly discusses the relaxation oscillations generated by system (2.2) with weak Allee effect ($A < 0$).

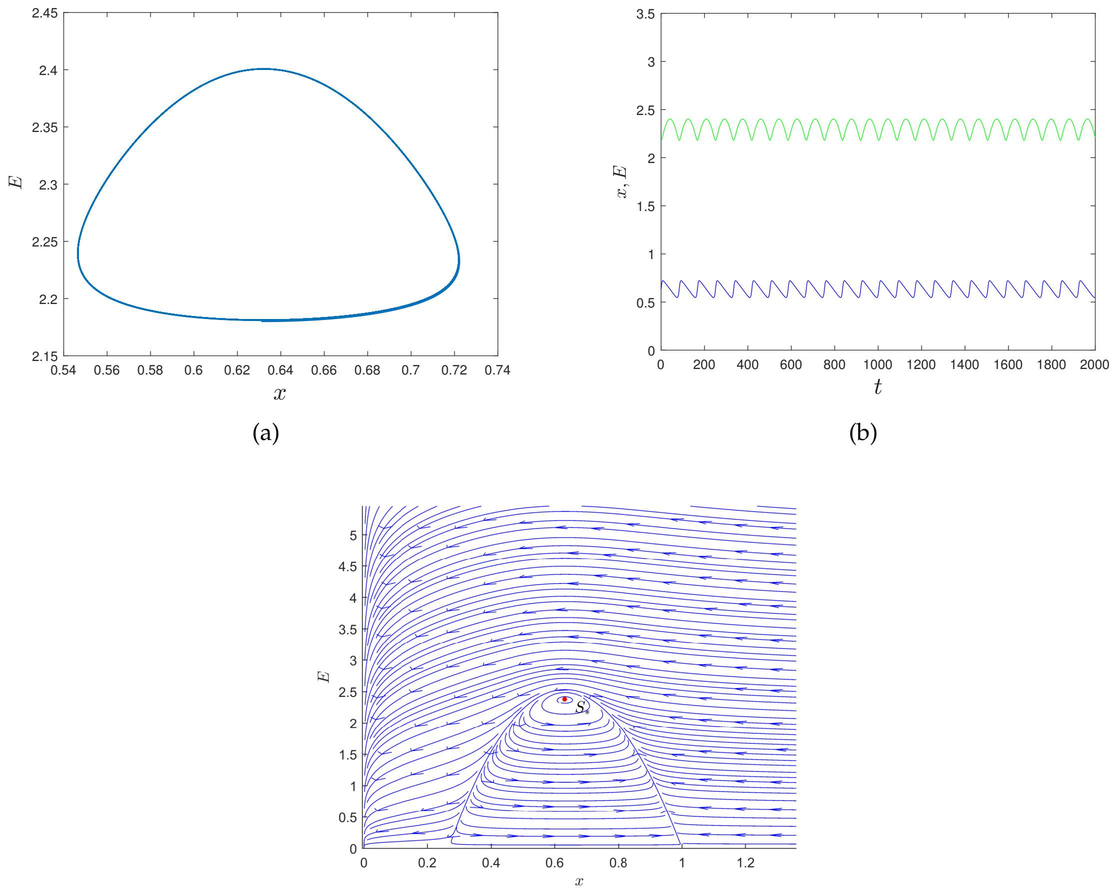

(a) (b) (c)

Figure 4.2: Phase plane analysis of system (2.2) for $\varepsilon = 0.05$ and $c = 2.8446$. (a) The canard without head generated by the system (2.2), when $K = 3$, $A = 0.8$, $\alpha = 0.17$, $\varepsilon = 0.05$, $\beta = 1.5$, $p = 3$, $c = 2.8446$. (b) $x - t$ (blue) and $E - t$ (green) time series diagram. (c) The phase diagram.

To discuss the existence of relaxation oscillations when $0 < x_* < x_f$, system (2.2) is expressed as follows:

$$\begin{cases} \dfrac{dx}{dt} = x f_1(x, E, \varepsilon), \\ \dfrac{dE}{dt} = \varepsilon g(x, E, \varepsilon), \end{cases} \tag{4.10}$$

where $(x, E) \in \mathbb{R}^2_+, 0 < \varepsilon \ll 1, f_1(x, E, \varepsilon) = (1 - x)(Kx - A) - \alpha E$ and $g(x, E, \varepsilon) = (\beta p x - c) E$. f_1 and g are sufficiently smooth and satisfy the following conditions:

$$f_1(x, E, \varepsilon) < 0, \quad g(x, E, \varepsilon) < 0, \quad \text{for } E > E_B > 0,$$
$$f_1(x, E, \varepsilon) > 0, \quad \text{for } E < E_B.$$

For $\varepsilon = 0$, the E-axis consists of the attracting part with $E > E_B$ and the repelling part with $E < E_B$. For a very small ε ($\varepsilon > 0$), the trajectory that starts from the point (x_0, E_0) ($x_0 > 0$ is quite small, $E > E_B$) gets attracted to the E-axis. Subsequently, it drifts downwards, and when it passes through $E = E_B$, it is repelled outside the E-axis. For a very small $\varepsilon(\varepsilon > 0)$, the trajectory intersects again with the line $x = x_0$ at the point whose E-coordinate value is $m_\varepsilon(E_0)$, such that $\lim_{\varepsilon \to 0} m_\varepsilon(E_0) = m_0(E_0)$, where $m_0(E_0)$ is is calculated by the following integration:

$$\int_{E_0}^{m_0(E_0)} \frac{f_1(0,E,0)}{g(0,E,0)} dE = 0. \tag{4.11}$$

The function $E_0 \to m_0(E_0)$ implicitly defined above is called the entry-exit function [8,37](see Figure 4.3).

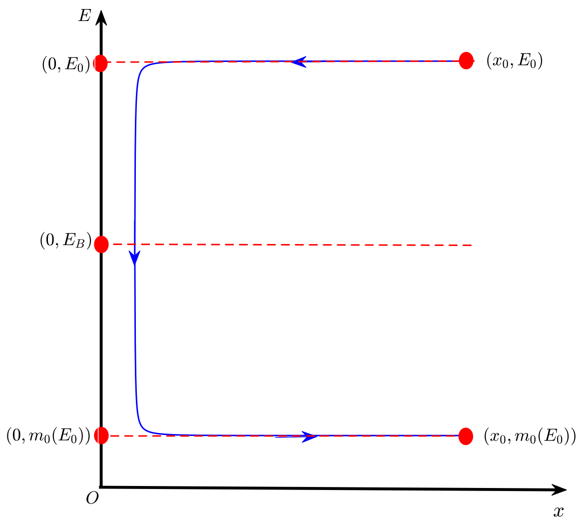

Figure 4.3: The entry-exit function. For system (2.2), when $\varepsilon = 0$, the branch of the E-axis is composed of the attracting part of $E > E_B$ and the repelling part of $E < E_B$. When $0 < \varepsilon \ll 1$, a typical orbit of system (2.2) starts at (x_0, E_0), where $E_0 > E_B$, and $x_0 > 0$ is very small, is attracted to the E-axis (not crossing the E-axis), gradually moves downwards along the E-axis until it reaches near $(0, m_0(E_0))$. Then it is repelled by the E-axis, and ends at point $(x_0, m_0(E_0))$.

On the basis of this, we have obtained the following results:

Lemma 4.3. *There exists a unique $\tilde{E}$ where $0 < \tilde{E} < -\frac{A}{\alpha}$, such that*

$$G(E) = \int_{E_f}^{E} \frac{f_1(0,s,0)}{g(0,s,0)} ds = 0. \tag{4.12}$$

Proof. We have

$$\begin{aligned} G(E) &= \int_{E_f}^{E} \frac{f_1(0,s,0)}{g(0,s,0)} ds \\ &= \int_{E_f}^{E} \frac{A+\alpha s}{cs} ds \\ &= \frac{A}{c} \ln \frac{E}{E_f} + \frac{\alpha}{c}(E - E_f) \to +\infty \quad \text{as } E \to 0^+. \end{aligned} \tag{4.13}$$

Furthermore, it can be calculated that

$$G'(E) = \frac{A+\alpha s}{cs}, \quad \text{for } 0 < E < -\frac{A}{\alpha}. \tag{4.14}$$

Therefore, G_E is strictly monotonically decreasing when $0 < E < -\frac{A}{\alpha}$. Again,

$$G\left(-\frac{A}{\alpha}\right) = \int_{E_f}^{-\frac{A}{\alpha}} \frac{A+\alpha s}{cs} ds < 0. \tag{4.15}$$

Thus there exists a unique $\tilde{E}$ where $0 < \tilde{E} < -\frac{A}{\alpha}$, such that $G(\tilde{E}) = 0$. □

The points $P(x_f, E_f)$ and $B(0, E_B)$ on the critical manifolds C_{10} and C_{20} that lose their hyperbolic properties are fold point and transcritical point, respectively. For fold point $P(x_f, E_f)$, we have

$$\frac{\partial f}{\partial E}|_{P(x_f,E_f)} = -\alpha x_f \neq 0,$$

as $c < \frac{(A+K)\beta p}{2K}$ and $g(x_f, E_f) \neq 0$ as $0 < x_* < x_f$. In addition, we have

$$\frac{\partial f}{\partial x^2}|_{P(x_f,E_f)} = -6Kx_f + 2(A+K) \neq 0,$$

consequently, $P(x_f, E_f)$ is a generic fold point as well as also a jump point, at which point the fast fiber flow leaves the critical manifold C_{20}.

For the transcritical point $B(0, E_B)$, we have

$$\begin{aligned} \frac{\partial f}{\partial x}|_{B(0,E_B)} &= 0, \\ \frac{\partial f}{\partial E}|_{B(0,E_B)} &= 0, \\ g(0, E_B) &= \frac{Ac}{\alpha} < 0, \\ \begin{vmatrix} \frac{\partial^2 f}{\partial x^2} & \frac{\partial^2 f}{\partial x \partial E} \\ \frac{\partial^2 f}{\partial x \partial E} & \frac{\partial^2 f}{\partial E^2} \end{vmatrix}_{B(0,E_B)} &= -\alpha^2 < 0, \end{aligned}$$

therefore, $B(0, E_B)$ is a generic transcritical point and jump point, at which point the fast flow is removed from the critical manifold C_{20}.

Define a singular fast-slow cycle Γ_0: the trajectory starts from $A(0, E_f)$, follows the slow flow along the E-axis to $C(0, \tilde{E})$. At $C(0, \tilde{E})$, it is repelled to the right, following the fast flow until it intersects with the attraction branch at point $D(\tilde{x}, \tilde{E})$. Then it follows the slow flow C_{20}^a to point $P(x_f, E_f)$, and finally follows the fast flow to the left back to point $A(0, E_f)$. Therefore, Γ_0 has four singular orbits, where $P(x_f, E_f)$ and $B(0, E_B)$ is the jump point, $A(0, E_f)$ and $D(\tilde{x}, \tilde{E})$ is the drop point (as shown by the red line in Figure 4.4).

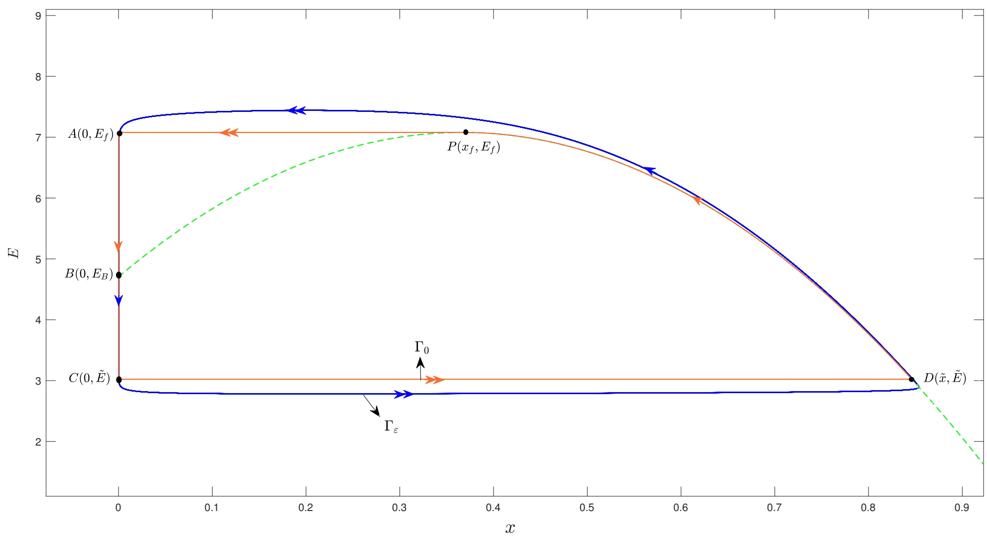

Figure 4.4: Representation the singular orbit Γ_0(red) and the relaxation oscillation orbit Γ_ε(blue) when $\varepsilon > 0$. The critical manifold of system (2.2) is represented by a green dashed line. Point $P(x_f, E_f)$ represents the maximum point of curve $E = u_0(x)$. The intersection point between curve $E = u_0(x)$ and the E-axis is $B(0, E_B)$. The branch on the E-axis is hyperbolic attracting with $E > E_B$ and The branches on the E-axis are hyperbolic repelling with $E < E_B$. The branch between P and B is hyperbolic repelling, while the right half branch of P is hyperbolic attracting. Double arrows denote fast flow. Single arrows denote slow flow.

Theorem 4.4. *If $\frac{A}{K} < \frac{c}{\beta p} < 1$, $c < \frac{(A+K)\beta p}{2K}$ and U is a small neighborhood of Γ_0 for system* (2.2)*. Then, for any sufficiently small $\varepsilon > 0$, there exists a unique limit cycle $\Gamma_\varepsilon \in U$. The limit cycle Γ_ε i attracting, and its characteristic multiplier is bounded by $-C/\varepsilon$ for a constant $C > 0$. Moreover, the limit cycle Γ_ε converges to Γ_0 in the Hausdoff distance when ε approaches 0.*

Proof. According to the Fenichel's theorem [9], $C^a_{10} = \{(x, E) \in \mathbb{R}^2_+, x = 0, E > -\frac{A}{\alpha}\}$ and $C^a_{20} = \{(x, E) \in \mathbb{R}^2_+, x_f < x < 1\}$ are the attracting part of the critical manifold, perturbing the nearby slow manifolds $C^a_{20,\varepsilon}$ and $C^a_{10,\varepsilon}$. By analyzing the dynamics near the fold point, the slow flow $C^a_{20,\varepsilon}$ follows the critical manifold C^a_{20} until it reaches the area near the generic fold point $P(x_f, E_f)$, and then jumps to another attracting branch C^a_{10}.

We consider a small cross-section Δ that intersects to C^a_{10} at a point between P and A, and track two trajectories Γ^1_ε and Γ^2_ε starting from Δ. According to the Fenichel's theorem [9] and Theorem 7.4.1 in [19], Γ^1_ε and Γ^2_ε will be attracted to the slow manifold C^a_{10} at an exponential velocity $\mathcal{O}(e^{\frac{1}{\varepsilon}})$. When passing through the generic transcritical point $B(0, E_B)$, $\Gamma^{1,2}_\varepsilon$ will contract exponentially with each other until they reach a neighborhood of $C^a_{20,\varepsilon}$. Applying Fenichel's theorem again, it is known that Γ^1_ε and Γ^2_ε will be attracted to the branch C^a_{20}, passing through point $P(x_f, E_f)$, and finally returning to A.

Therefore, we obtained a return map Σ: $\Delta \to \Delta$ induced by the flow of system (2.2) with $0 < \varepsilon \ll 1$. Σ is a compressed map when the trajectories contract with each other at a rate $\mathcal{O}(e^{\frac{1}{\varepsilon}})$. According to the principle of compression map, Σ has a unique stable fixed point, which is the expected limit cycle Γ_ε(As shown by the blue line in Figure 4.4). Since contraction is exponential, the characteristic multiplier of Γ_ε has an upper bound of $-C/\varepsilon$ for $C > 0$. Applying the Fenichel's theorem [9] and Theorem 7.4.1 in [19], it is obtained that the limit cycle Γ_ε converges to Γ_0 in the Hausdoff distance when $\varepsilon \to 0$. □

Remark 4.5. For the fishery economy, relaxation oscillations usually rotate counterclockwise. This is due to the input of food by the aquaculture plant, which leads to an increase in fish density. After the increase in fish density, the workload for catching also increases. Correspondingly, as the amount of capture effort increases, the density of fish schools will also decrease. As the number of fish schools decreases, the workload for catching will also decrease. After going through these steps, the system returned to its initial state and continued to oscillate counterclockwise. This means that the system is in a dynamic equilibrium, with a focus on the capture effort increasing at a slow time scale compared to fish density. For aquaculture, this means that its economy is turnover, allowing for optimized resource allocation and sustained economic activities.

4.4 Stochastic differential system

In nature, biological populations are inevitably subject to random disturbances from the external environment, such as storms, earthquakes, natural enemies, etc. Similarly, the capture of population is also affected by weather and natural disasters. Therefore, a random perturbation term is added to discuss the existence of stationary distribution of the system's solution. We assume that the random disturbance is white noise type, which is proportional to x and E in system (2.2). Therefore, the system with added random disturbance is described as:

$$\begin{cases} dx = [x(1-x)(Kx-A) - \alpha E x]dt + \sigma_f x dB_1(t) = f(x,E)dt + \sigma_f x dB_1(t), \\ dE = \varepsilon(\beta p x - c)E dt + \sqrt{\varepsilon}\sigma_g E dB_2(t) = \varepsilon g(x,E)dt + \sqrt{\varepsilon}\sigma_g E dB_2(t). \end{cases} \tag{4.16}$$

Perform a time scale transformation of $\tau = \varepsilon t$, the above equation is transformed into

$$\begin{cases} dx = \dfrac{1}{\varepsilon}[x(1-x)(Kx-A) - \alpha E x]d\tau + \dfrac{\sigma_f x}{\sqrt{\varepsilon}} dB_1(\tau) = \dfrac{1}{\varepsilon} f(x,E)dt + \dfrac{\sigma_f x}{\sqrt{\varepsilon}} dB_1(\tau), \\ dE = (\beta p x - c)E d\tau + \sigma_g E dB_2(\tau) = g(x,E)d\tau + \sigma_g E dB_2(\tau), \end{cases} \tag{4.17}$$

where $B_i(\tau)$, $i = 1,2$ is the standard Brownian motion on a complete probability space $(\Omega, \mathcal{F}, \mathbb{P})$, σ_f and σ_g represents noise intensity.

Theorem 4.6. *For any $(x(0), E(0)) \in \mathbb{R}_+^2$, as $\varepsilon \to 0$, solution of (4.17) converges weakly to $E(\cdot)$ that is a solution of the stochastic differential equation*

$$dE(\tau) = \left(\beta p E \int_{x(0)}^{\infty} x \mu_E(x) dx - cE\right) d\tau + \sigma_g E dB_2(\tau). \tag{4.18}$$

Proof. According to [17], we need to calculate the invariant measure $\mu_{\bar{E}}(x)$ of equation (4.17)-1, that is, to calculate the Fokker–Planck equation corresponding to equation (4.17)-1:

$$\frac{\partial P(x,\tau|E)}{\partial \tau} = -\frac{\partial}{\partial x}\left\{\frac{1}{\varepsilon}\left(x(1-x)(Kx-A) - \alpha E x\right) p(x,\tau|E)\right\} + \frac{1}{2}\frac{\partial^2}{\partial x^2}\left(\frac{\sigma_f^2 x^2}{\varepsilon} p(x,\tau|E)\right) = 0.$$

By transforming $\tau = \varepsilon t$, the above equation is transformed into

$$\frac{\partial P(x,t|E)}{\partial t} = -\frac{\partial}{\partial x}\left\{\left(x(1-x)(Kx-A) - \alpha E x\right) p(x,t|E)\right\} + \frac{1}{2}\frac{\partial^2}{\partial x^2}\left(\sigma_f^2 x^2 p(x,t|E)\right).$$

Solving $\frac{\partial P(x,t|E)}{\partial t} = 0$, we obtain

$$\mu_E(x) = Cx^{-N} \exp\left\{ \frac{2(K+A)}{\sigma_f^2} x - \frac{K}{\sigma_f^2} x^2 \right\},$$

where $N = \frac{2(A+\alpha E)}{\sigma_f^2} + 2$, C is a normalization constant that satisfies

$$C \int_{x(0)}^{\infty} x^{-N} \exp\left\{ \frac{2(K+A)}{\sigma_f^2} x - \frac{K}{\sigma_f^2} x^2 \right\} dx = 1.$$

To ensure that C is computable, we prove that the integral $\int_{x(0)}^{\infty} x^{-N} \exp\left\{ \frac{2(K+A)}{\sigma_f^2} x - \frac{K}{\sigma_f^2} x^2 \right\} dx$ converges. For the proof of integral convergence, please refer to the appendix.

According to the Khasminskii's limit theorem [16] and Theorem 5.1 in [40], in the extreme case $\varepsilon \to 0$, the evolution of the slow variable E can be described by a simplified stochastic differential equation, as follows

$$dE(\tau) = g_{red}(E)d\tau + \sigma_{red}(E)dB_2(\tau), \tag{4.19}$$

where

$$g_{red}(E) = \int_{x(0)}^{\infty} (\beta p x - c) E \mu_E(x) dx,$$
$$\sigma_{red}^2(E) = \int_{x(0)}^{\infty} \sigma_g^2 E^2 \mu_E(x) dx.$$

Since $\int_{x(0)}^{\infty} \mu_E(x) dx = 1$, we obtain that

$$g_{red}(E) = \beta p E \int_{x(0)}^{\infty} x \mu_E(x) dx - cE,$$
$$\sigma_{red}^2(E) = \sigma_g^2 E^2.$$

Therefore, $\sigma_{red}(E) = \sigma_g E$,

$$\int_0^{\infty} x \mu_E(x) dx = \frac{\int_{x(0)}^{\infty} x^{-N+1} \exp\left\{ \frac{2(K+A)}{\sigma_f^2} x - \frac{K}{\sigma_f^2} x^2 \right\} dx}{\int_{x(0)}^{\infty} x^{-N} \exp\left\{ \frac{2(K+A)}{\sigma_f^2} x - \frac{K}{\sigma_f^2} x^2 \right\} dx}.$$

Similarly, we also need to prove that $\int_{x(0)}^{\infty} x^{-N+1} \exp\left\{ \frac{2(K+A)}{\sigma_f^2} x - \frac{K}{\sigma_f^2} x^2 \right\} dx$ is convergent, as shown in the appendix. Furthermore, substituting $g_{red}(E)$ and $\sigma_{red}(E)$ into eq. (4.19), we have

$$dE(\tau) = \left(\beta p E \int_{x(0)}^{\infty} x \mu_E(x) dx - cE \right) d\tau + \sigma_g E dB_2(\tau).$$

$\square$

Theorem 4.7. *System* (4.18) *has a globally unique positive solution, for any initial value* $(x(0), E(0)) \in \mathbb{R}_+^2$.

Proof. We verify the existence and uniqueness of the global positive solution by proving that system(4.18) satisfies the Lipschitz condition and linear growth condition.

Taking $L = \left|\beta p(\int_{x(0)}^{\infty} x\mu_E(x)dx)\right| + |c| + |\sigma_g|$, and we calculate that

$$\begin{aligned}
&|g_{red}(E_1) - g_{red}(E_2)| + |\sigma_{red}(E_1) - \sigma_{red}(E_2)| \\
&= \left|\beta p(\int_{x(0)}^{\infty} x\mu_E(x)dx) - c\right| |E_1 - E_2| + |\sigma_g||E_1 - E_2| \\
&= \left(\left|\beta p(\int_{x(0)}^{\infty} x\mu_E(x)dx) - c\right| + |\sigma_g|\right) |E_1 - R_2| \\
&\leqslant \left(\left|\beta p(\int_{x(0)}^{\infty} x\mu_E(x)dx)\right| + |c| + |\sigma_g|\right) |E_1 - E_2| \leqslant L|E_1 - E_2|,
\end{aligned}$$

and

$$\begin{aligned}
|g_{red}(E)| + |\sigma_{red}(E)| &= \left(\left|\beta p(\int_{x(0)}^{\infty} x\mu_E(x)dx) - c\right| + |\sigma_g|\right) |E| \\
&\leqslant \left(\left|\beta p(\int_{x(0)}^{\infty} x\mu_E(x)dx)\right| + |c| + |\sigma_g|\right) |E| \\
&\leqslant L(1 + |E|).
\end{aligned}$$

Therefore, the Lipschitz condition and linear growth condition are satisfied. □

Theorem 4.8. *For any $(x(0), E(0)) \in \mathbb{R}_+^2$, if $2\beta p \int_{x(0)}^{\infty} x\mu_E(x)dx < \sigma_g^2 + 2c$ is met, the system (4.18) exhibits a stationary distribution.*

Proof. The FPK equation for system (4.18) is

$$\frac{\partial P(E)}{\partial \tau} = \frac{\partial}{\partial E}\left(\beta p E \int_{x(0)}^{\infty} x\mu_E(x)dx - cE\right) p(E) + \frac{1}{2}\frac{\partial^2}{\partial E^2}\sigma_g^2 E^2 p(E).$$

In order to obtain the probability density function of the stationary distribution of $E(\tau)$, we need to solve for $\frac{\partial P(E)}{\partial \tau} = 0$. The calculated result is as follows

$$p(E) = ME^{-\frac{2\sigma_g^2 - 2\left(\beta p \int_{x(0)}^{\infty} x\mu_E(x)dx - c\right)}{\sigma_g^2}},$$

where M is a normalization constant.

Below we prove that $\int_{E(0)}^{+\infty} p(E)dE = 1$ which is holds, it indicates the existence of the probability density function of $E(\tau)$, which also proves the existence of a stationary distribution for system (4.18).

We prove that the integral

$$\int_{E(0)}^{+\infty} E^{-\frac{2\sigma_g^2 - 2\left(\beta p \int_{x(0)}^{\infty} x\mu_E(x)dx - c\right)}{\sigma_g^2}} dE$$

is convergent. Based on the condition

$$2\beta p \int_{x(0)}^{\infty} x\mu_E(x)dx < \sigma_g^2 + 2c,$$

we obtain

$$-\frac{2\sigma_g^2 - 2\left(\beta p \int_{x(0)}^{\infty} x\mu_E(x)dx - c\right)}{\sigma_g^2} > 1.$$

According to the convergence rule of integrals, when $-\frac{2\sigma_g^2-2\left(\beta p\int_{x(0)}^{\infty}x\mu_E(x)dx-c\right)}{\sigma_g^2}>1$, the integral is convergent. At this point, there must exist a constant M that makes $\int_{E(0)}^{+\infty}p(E)dE=1$. Thus, Theorem 4.8 is proven. □

Remark 4.9. Calculating the integral $\int_{x(0)}^{\infty}x^{-N}\exp\left\{\frac{2(K+A)}{\sigma_f^2}x-\frac{K}{\sigma_f^2}x^2\right\}dx$ is too complex, and we have not provided an exact solution for the integral here. We have only proven that the integral is convergent. For more accurate results, one can use Matlab or Maple to find its numerical solution.

5 Stochastic model with weak Allee effect

In this section, we consider the time scale parameter ε as a regular parameter and discuss the stochastic behavior of the system (4.17). We discussed the existence of a stationary distribution for system (4.17) and the stochastic bifurcation of the system (4.17).

5.1 Existence and uniqueness of global positive solutions

When discussing the dynamic behavior of biological systems, the first thing we need to focus on is whether the system has a global positive solution. So we presented the theorem about the existence of a unique global positive solution for system (4.17):

Theorem 5.1. *Let $-K<A<0$, for any initial value taken from $(x(0),E(0))\in\mathbb{R}_+^2$, system (4.17) has a unique global positive solution $(x(\tau),E(\tau))$(where $\tau\geq 0$). And the solution is always within $\mathbb{R}_+^2$ with probability 1, which means that for any $\tau\geq 0$, $(x(\tau),E(\tau))\in\mathbb{R}_+^2$ almost surely (a.s.).*

Proof. For any initial value $(x(0),E(0))\in\mathbb{R}_+^2$, the system always has a solution $(x(\tau),E(\tau))\in\mathbb{R}_+^2$ at $t\in[0,\tau_e)$, τ_e is the moment of explosion. To prove that the solution is a global solution, it is only necessary to prove that $\tau_e=\infty$ a.s. Assuming that $n_0\geq 1$ is sufficiently large such that $(x(0),E(0))\in(\frac{1}{n_0},n_0)$. For any integer $n>n_0$, define the stopping time:

$$\tau_n=\inf\left\{\tau\in(0,\tau_e):\min\{x(\tau),E(\tau)\}\leq\tfrac{1}{n}\text{ or }\max\{x(\tau),E(\tau)\}\geq n\right\},$$

where we assume that $inf\,\emptyset=\infty$ in this article (as is common, $\emptyset$ denotes the empty set). Obviously, τ_n monotonically increases when $n\to\infty$. Let $\tau_\infty=\lim_{n\to\infty}\tau_n$, where $\tau_\infty\leq\tau_n$ a.s. If $\tau_\infty=\infty$ a.s. holds, then $\tau_e=\infty$ a.s also holds, and there is $(x(\tau),E(\tau))\in\mathbb{R}_+^2$ for all $\tau\geq 0$, so we only need to prove that $\tau_\infty=\infty$ a.s. Otherwise, there will be a pair of constants $T>0$, $\eta\in(0,1)$, such that $P\{\tau_n\leq T\}>\eta$. Therefore, there is an integer $n_1\geq n_0$ such that $P\{\tau_n\leq T\}\geq\eta$ for all $n>n_1$.

Define a C^2-function $V:\mathbb{R}_+^2\to\mathbb{R}$ by

$$V(x(\tau),E(\tau))=x-a-a\ln\frac{x}{a}+b(E-1-\ln E),\tag{5.1}$$

where a and b are positive constants, it is easy to obtain that $V(x,E)$ is a nonnegative function. Using Itô's formula, we obtain

$$dV(x,E)=LV(x,E)d\tau+\frac{\sigma_f}{\sqrt{\varepsilon}}(x-a)dB_1(\tau)+b\sigma_g(E-1)dB_2(\tau),\tag{5.2}$$

where $LV(x,E)$: $\mathbb{R}_+^2 \to \mathbb{R}$ is defined as follows:

$$\begin{aligned} LV(x,E) = & -\frac{K}{\varepsilon}x^3 + \frac{A+K}{\varepsilon}x^2 - \frac{A}{\varepsilon}x + \frac{\alpha}{\varepsilon}xE + \frac{\alpha K}{\varepsilon}x^2 - \frac{\alpha(A+K)}{\varepsilon}x \\ & + \frac{aA}{\varepsilon} + \frac{\alpha a}{\varepsilon}E + b\beta pxE - bcE - b\beta px + bc + \frac{a\sigma_f^2}{2\varepsilon} + \frac{b\sigma_g^2}{2} \\ = & -\frac{K}{\varepsilon}x^3 + \frac{A+K+aK}{\varepsilon}x^2 - \frac{A+a(A+K)+b\varepsilon\beta p}{\varepsilon}x \\ & + \left(\frac{\alpha a}{\varepsilon} - bc\right)E + \left(b\beta p - \frac{\alpha}{\varepsilon}\right)xE + \frac{aA}{\varepsilon} + bc + \frac{a\sigma_f^2}{2\varepsilon} + \frac{b\sigma_g^2}{2}, \end{aligned}$$

Take $a = \frac{c}{\beta p}$, $b = \frac{\alpha}{\varepsilon\beta p}$, so that $\frac{\alpha a}{\varepsilon} - bc = 0$ and $b\beta p - \frac{\alpha}{\varepsilon} = 0$, then

$$\begin{aligned} LV(x,E) = & -\frac{K}{\varepsilon}x^3 + \frac{A+K+aK}{\varepsilon}x^2 - \frac{A+a(A+K)+b\varepsilon\beta p}{\varepsilon}x + \frac{aA}{\varepsilon} + bc + \frac{a\sigma_f^2}{2\varepsilon} + \frac{b\sigma_g^2}{2} \\ \le & \, b_1 + \frac{aA}{\varepsilon} + bc + \frac{a\sigma_f^2}{2\varepsilon} + \frac{b\sigma_g^2}{2} =: M, \end{aligned}$$

where $b_1 = \sup_{x\in(0,+\infty)}\left\{-\frac{K}{\varepsilon}x^3 + \frac{A+K+aK}{\varepsilon}x^2 - \frac{A+a(A+K)+b\varepsilon\beta p}{\varepsilon}x\right\}$, M is a constant. Then we can obtain

$$dV(x,E) \le Md\tau + \frac{\sigma_f}{\sqrt{\varepsilon}}(x-a)dB_1(\tau) + b\sigma_g(E-1)dB_2(\tau). \tag{5.3}$$

Integrating from 0 to $\tau_n \wedge T$ at both sides of (5.3), we have:

$$\begin{aligned} V(x(\tau_n\wedge T), E(\tau_n\wedge T)) \le & \, V(x(0),E(0)) + M(x(\tau_n\wedge T)) \\ & + \int_0^{\tau_n\wedge T}\frac{\sigma_f}{\sqrt{\varepsilon}}(x-a)dB_1(\tau) + b\int_0^{\tau_n\wedge T}\sigma_g(E-1)dB_2(\tau). \end{aligned}$$

By taking the expected values from both sides of the above equation, we can obtain

$$\begin{aligned} EV(x(\tau_n\wedge T), E(\tau_n\wedge T)) & \le V(x(0),E(0)) + ME(\tau_n\wedge T) \\ & \le V(x(0),E(0)) + MT. \end{aligned} \tag{5.4}$$

Therefore, let $\Omega_n = \{\omega\in\Omega, \tau_n = \tau_n(\omega) \le T\}$, it can be obtained that $P(\Omega_n) > \eta$ for all $n \ge n_0$. For each $\omega \in \Omega_n$, $x(\tau,\omega)$ and $E(\tau,\omega)$ have at least one equal to n or $\frac{1}{n}$, then we get

$$\begin{aligned} & V(x(0),E(0)) + MT \\ & \quad \ge E(I_{\Omega_n}V(x(\tau_n,\omega),E(\tau_n,\omega)) \\ & \quad \ge \eta\left[b(n-1-\ln n)\wedge b\left(\frac{1}{n}-1-\ln\frac{1}{n}\right)\wedge\left(n-a-a\ln\frac{n}{a}\right)\wedge\left(\frac{1}{n}-a+\ln an\right)\right], \end{aligned}$$

where $I_{\Omega_n(\omega)}$ is the indicative function of Ω_n. If $n\to\infty$, a contradiction arises where $\infty > V(x(0),E(0)) + MY = \infty$. Therefore, there is $\tau_\infty = \infty$ a.s. □

5.2 Stationary distribution and ergodic properties

A stationary distribution is characterized by the fluctuation of the solution of a stochastic system within a certain neighborhood of the positive equilibrium point of the corresponding deterministic system and can be regarded as weak stability. Next, we provide sufficient conditions for the existence of a stationary distribution in system (4.17).

Theorem 5.2. *Assuming* $\frac{\varepsilon(A+\frac{\sigma_f^2}{2})}{\alpha} < \frac{c+\frac{\sigma_g^2}{c}}{c}$, $\varepsilon < \alpha c$ *and* $\beta p < \frac{1}{\varepsilon}$, *the system* (4.17) *has a stationary distribution and it has the ergodic property for any initial value* $(x(0), E(0)) \in \mathbb{R}_+^2$.

Proof. Define C^2-function V_1 as follows:

$$V_1(x,E) = v(x,E) + \alpha k E - v(x_1, E_1),$$

where $v(x,E) = kx - \frac{\varepsilon^2 k}{\alpha}\ln x + \frac{k}{c}\ln E + \frac{1}{E^\rho}$, k and $\rho(0<\rho<1)$ are positive numbers, $(x_1, E_1) = (\frac{\varepsilon^2}{\alpha}, (\frac{k}{c\rho})^{-\frac{1}{\rho}})$ is the minimum value point of $v(x,E)$.

Using Itô's formula, we get

$$\begin{aligned} LV_1 = &\frac{k}{\varepsilon}[x(1-x)(Kx-A) - \alpha x E] - \frac{\varepsilon k}{\alpha}[(1-x)(Kx-A) - \alpha E] \\ &+ \frac{k}{c}(\beta p x - c) - \rho E^{-\rho}(\beta p x - c) + \alpha k(\beta p x - c)E + \frac{k\varepsilon\sigma_f^2}{2\alpha} - \frac{k\sigma_g^2}{2c} + \frac{1}{2}\rho(\rho+1)\sigma_g^2 E^{-\rho} \\ = & - \frac{kK}{\varepsilon}x^3 + \frac{\alpha k(A+K) + \varepsilon^2 kK}{\alpha\varepsilon}x^2 - \frac{\varepsilon k(A+K)}{\alpha}x - \frac{kA}{\varepsilon}x + \frac{k\beta p}{c}x \\ &- k(\alpha c - \varepsilon)E - k\left(\frac{\alpha}{\varepsilon} - \alpha\beta p\right)xE - \rho\beta p x E^{-\rho} + \rho E^{-\rho}\left(c + \frac{1}{2}\rho(\rho+1)\sigma_g^2\right) \\ &- k\left(\frac{(c+\frac{\sigma_g^2}{2})}{c} - \frac{\varepsilon(A+\frac{\sigma_f^2}{2})}{\alpha}\right). \end{aligned} \tag{5.5}$$

Considering a bounded closed set

$$U_{\eta_1} = \left\{(x,E) \in \mathbb{R}_+^2, \eta_1 \le x \le \frac{1}{\eta_1}, \eta_1 \le E \le \frac{1}{\eta_1}\right\}.$$

Furthermore, we can obtain

$$\mathbb{R}_+^2 \setminus U_{\eta_1} = U_1 \cup U_2 \cup U_3 \cup U_4,$$

where

$$U_1 = \left\{(x,E) \in \mathbb{R}_+^2, E > \frac{1}{\eta_1}\right\}; \qquad U_2 = \left\{(x,E) \in \mathbb{R}_+^2, 0 < x < \eta_1\right\};$$
$$U_2 = \left\{(x,E) \in \mathbb{R}_+^2, 0 < E < \eta_1\right\}; \qquad U_4 = \left\{(x,E) \in \mathbb{R}_+^2, x > \frac{1}{\eta_1}\right\}.$$

We choose $\eta_1 > 0$ as a sufficiently small constant and satisfy the following conditions:

$$B_1 - k(\alpha c - \varepsilon)\frac{1}{\eta_1} + \rho\eta_1^\rho(c + \frac{1}{2}(\rho+1)\sigma_g^2) \le -1, \tag{5.6}$$

$$\frac{2\beta p \eta_1}{c\left(\frac{c+\frac{\sigma_g^2}{2}}{c} - \frac{\varepsilon(A+\frac{\sigma_f^2}{2})}{\alpha}\right)} < \frac{1}{2}, \tag{5.7}$$

$$\frac{2\varepsilon\eta_1}{\frac{c+\frac{\sigma_g^2}{2}}{c} - \frac{\varepsilon(A+\frac{\sigma_f^2}{2})}{\alpha}} < \frac{1}{2}, \tag{5.8}$$

$$D_1 - \frac{\alpha k(A+K) + \varepsilon^2 kK}{\alpha\varepsilon\eta_1} < -1, \tag{5.9}$$

where B_2 and D_2 are positive constants that can be determined from the following inequalities (5.10), (5.12). Next, we prove that LV_1 is negative in regions U_i, $i = 1,2,3,4$.

Case 1: If $(x,E) \in U_1$, we have

$$\begin{aligned} LV_1 \leq & -\frac{kK}{\varepsilon}x^3 + \frac{\alpha k(A+K)+\varepsilon^2 kK}{\alpha\varepsilon}x^2 - \frac{\alpha kA + \varepsilon^2 k(A+K)}{\alpha\varepsilon}x \\ & + \frac{k\beta p}{c}x - k(\alpha c - \varepsilon)E + \rho E^{-\rho}\left(c + \frac{1}{2}\rho(\rho+1)\sigma_g^2\right) \\ \leq & B_1 - k(\alpha c-\varepsilon)E + \rho E^{-\rho}\left(c + \frac{1}{2}\rho(\rho+1)\sigma_g^2\right) \\ \leq & B_1 - k(\alpha c - \varepsilon)\frac{1}{\eta_1} + \rho\eta_1^{\rho}\left(c + \frac{1}{2}\rho(\rho+1)\sigma_g^2\right), \end{aligned} \tag{5.10}$$

where

$$B_1 = \sup_{x\in(0,+\infty)}\left\{-\frac{kK}{\varepsilon}x^3 + \frac{\alpha k(A+K)+\varepsilon^2 kK}{\alpha\varepsilon}x^2 - \frac{\alpha kA+\varepsilon^2 k(A+K)}{\alpha\varepsilon}x + \frac{k\beta p}{c}x\right\}.$$

According to condition (5.6), we can obtain that $LV_1 \leq -1$ on U_1.

Case 2: If $(x,E) \in U_2$, one can see that

$$\begin{aligned} LV_1 \leq & -\frac{kK}{\varepsilon}x^3 + \frac{\alpha k(A+K)+\varepsilon^2 kK}{\alpha\varepsilon}x^2 - \frac{kA}{\varepsilon}x + \frac{k\beta p}{c}x - k(\alpha c-\varepsilon)E \\ & + \rho E^{-\rho}\left(c + \frac{1}{2}\rho(\rho+1)\sigma_g^2\right) - k\left(\frac{(c+\frac{\sigma_g^2}{2})}{c} - \frac{\varepsilon(A+\frac{\sigma_f^2}{2})}{\alpha}\right) + \frac{k\beta p}{c}x \\ \leq & C_1 - k\left(\frac{(c+\frac{\sigma_g^2}{2})}{c} - \frac{\varepsilon(A+\frac{\sigma_f^2}{2})}{\alpha}\right) + \frac{k\beta p}{c}x \\ \leq & C_1 - k\left(\frac{(c+\frac{\sigma_g^2}{2})}{c} - \frac{\varepsilon(A+\frac{\sigma_f^2}{2})}{\alpha}\right) + \frac{k\beta p}{c}\eta_1, \end{aligned} \tag{5.11}$$

where

$$\begin{aligned} C_1 = \sup_{(x,E)\in\mathbb{R}_+^2} & \left\{-\frac{kK}{\varepsilon}x^3 + \frac{\alpha k(A+K)+\varepsilon^2 kK}{\alpha\varepsilon}x^2 - \frac{kA}{\varepsilon}x + \frac{k\beta p}{c}x \right. \\ & \left. -k(\alpha c-\varepsilon)E + \rho E^{-\rho}\left(c+\frac{1}{2}\rho(\rho+1)\sigma_g^2\right)\right\}. \end{aligned}$$

If we choose $k = \frac{2C_1}{\frac{(c+\frac{\sigma_g^2}{2})}{c} - \frac{\varepsilon(A+\frac{\sigma_f^2}{2})}{\alpha}}$, we can obtain

$$LV_1 \leq -C_1 + \frac{2\beta p C_1 \eta_1}{c\left(\frac{(c+\frac{\sigma_g^2}{2})}{c} - \frac{\varepsilon(A+\frac{\sigma_f^2}{2})}{\alpha}\right)}.$$

It follows from (5.7), we can obtain $LV_1 \leq -\frac{C_1}{2}$ on U_2.

Case 3: If $(x,E)\in U_3$, we have

$$\begin{aligned}LV_1 \le& -\frac{kK}{\varepsilon}x^3+\frac{\alpha k(A+K)+\varepsilon^2 kK}{\alpha\varepsilon}x^2-\frac{kA}{\varepsilon}x+\frac{k\beta p}{c}x-k(\alpha c-\varepsilon)E\\ &+\rho E^{-\rho}\left(c+\frac{1}{2}\rho(\rho+1)\sigma_g^2\right)-k\left(\frac{(c+\frac{\sigma_g^2}{2})}{c}-\frac{\varepsilon(A+\frac{\sigma_f^2}{2})}{\alpha}\right)+k\varepsilon E\\ \le& C_1-k\left(\frac{(c+\frac{\sigma_g^2}{2})}{c}-\frac{\varepsilon(A+\frac{\sigma_f^2}{2})}{\alpha}\right)+k\varepsilon E\\ \le& C_1-k\left(\frac{(c+\frac{\sigma_g^2}{2})}{c}-\frac{\varepsilon(A+\frac{\sigma_f^2}{2})}{\alpha}\right)+k\varepsilon\eta_1,\end{aligned}$$

where $k=\frac{2C_1}{\frac{(c+\frac{\sigma_g^2}{2})}{c})-\frac{\varepsilon(A+\frac{\sigma_f^2}{2})}{\alpha}}$, C_1 is given by (5.11), then we can obtain

$$LV_1\le -C_1+\frac{2\varepsilon C_1\eta_1}{c\left(\frac{(c+\frac{\sigma_g^2}{2})}{c}-\frac{\varepsilon(A+\frac{\sigma_f^2}{2})}{\alpha}\right)}.$$

According to condition (5.8), we can obtain $LV_1\le -\frac{C_2}{2}$ on U_3.

Case 4: If $(x,E)\in U_4$, one can see that

$$\begin{aligned}LV_1\le& -\frac{kK}{\varepsilon}x^3+\frac{\alpha k(A+K)+\varepsilon^2 kK}{\alpha\varepsilon}x^2-\frac{kA}{\varepsilon}x+\frac{k\beta p}{c}x-k(\alpha c-\varepsilon)E\\ &+\rho E^{-\rho}\left(c+\frac{1}{2}\rho(\rho+1)\sigma_g^2\right)-\frac{\alpha kA+\varepsilon^2k(A+K)}{\alpha\varepsilon}x\\ \le& D_1-\frac{\alpha kA+\varepsilon^2k(A+K)}{\alpha\varepsilon}x\\ \le& D_1-\frac{\alpha kA+\varepsilon^2k(A+K)}{\alpha\varepsilon\eta_1},\end{aligned}\tag{5.12}$$

where

$$D_1=\sup_{x\in(0,+\infty)}\left\{-\frac{kK}{\varepsilon}x^3+\frac{\alpha k(A+K)+\varepsilon^2 kK}{\alpha\varepsilon}x^2-\frac{kA}{\varepsilon}x+\frac{k\beta p}{c}x\right.$$
$$\left.-k(\alpha c-\varepsilon)E+\rho E^{-\rho}\left(c+\frac{1}{2}\rho(\rho+1)\sigma_g^2\right)\right\}.$$

According to condition (5.9), we can conclude that $LV_1\le -1$ on U_4. Thus we can obtain that for a enough small η, $LV_1\le -\max\{1,\frac{C_1}{2}\}$ for all $(x,E)\in\mathbb{R}_+^2\setminus U_{\eta_1}$.

In addition, the diffusion matrix of system (4.17) is

$$\begin{pmatrix}\frac{\sigma_f^2}{\varepsilon}x^2 & 0\\ 0 & \sigma_g^2E^2\end{pmatrix}.$$

Choose

$$M_1 = \min_{(x,E)\in\mathbb{R}_+^2\setminus U_{\eta_1}} \left\{ \frac{\sigma_f^2}{\varepsilon} x^2, \sigma_g^2 E^2 \right\},$$

we have

$$\frac{\sigma_f^2}{\varepsilon} x^2 \xi_1^2 + \sigma_g^2 E^2 \xi_2^2 \geq M_1 |\xi^2|, \ \ (x,E) \in \mathbb{R}_+^2 \setminus U_{\eta_1}, \ \ \xi = (\xi_1, \xi_2) \in \mathbb{R}_+^2.$$

Therefore, the system has a stationary distribution and it has the ergodic property. □

Combining Theorem 4.6 and 4.7, we can conclude that both the system (4.17) without random reduction and the system (4.18) after random reduction have globally unique positive solutions. And under certain conditions, they have stationary distribution.

Remark 5.3. The existence of a stationary distribution indicates that under current fishing and environmental conditions, fish populations can maintain a relatively healthy quantity state, which is conducive to the sustainable development of fisheries. For fisheries practitioners and managers, a stationary distribution is an important reference for formulating fishing strategies and fisheries management policies. It can help determine a reasonable fishing intensity to achieve a balance between economic and ecological benefits. If the stable distribution of fish populations indicates relatively abundant resources, then it is appropriate to reduce aquaculture inputs and increase fishing output; On the contrary, if the stable distribution shows that the resources are at an unstable or low level, it is necessary to increase aquaculture efforts and control fishing intensity to ensure the sustainable development of the fishery economy.

5.3 Stochastic stability

In this section, the stability and bifurcation behavior of the stochastic system (4.16) near its internal equilibrium point S_* will be discussed. In order to obtain stochastic differential equations in small parameter form, we introduce the following standard rescalings [26]:

$$K = \varepsilon\tilde{K}, \quad A = \varepsilon\tilde{A}, \quad \alpha = \varepsilon\tilde{\alpha}, \quad \sigma_f = \sqrt{\varepsilon}\tilde{\sigma}_f,$$

where $0 < \varepsilon \ll 1$ is the time scale parameter. And system (4.16) is transformed into:

$$\begin{cases} dx = \varepsilon[x(1-x)(\tilde{K}x - \tilde{A}) - \tilde{\alpha}Ex]dt + \sqrt{\varepsilon}\tilde{\sigma}_f x dB_1(t) =: \varepsilon \tilde{f}(x,E,\varepsilon)dt + \varepsilon\tilde{\sigma}_f x dB_1(t), \\ dE = \varepsilon(\beta p x - c)E dt + \sqrt{\varepsilon}\sigma_g E dB_2(t) =: \varepsilon g(x,E)dt + \sqrt{\varepsilon}\sigma_g E dB_2(t), \end{cases} \tag{5.13}$$

which system (5.13) is a regular stochastic differential equation. In order to better study the dynamic behavior near the equilibrium point $\tilde{S}_*(\tilde{x}_*, \tilde{E}_*)$ where $\tilde{x}_* = \frac{c}{\beta p}$, $w\tilde{E}_* = \frac{(1-\tilde{x}_*)(\tilde{K}\tilde{x}_* - \tilde{A})}{\tilde{\alpha}}$, we translate it to the origin and perform a polar coordinate transformation $x = \tilde{x}_* + r\cos\theta$, $E = \tilde{E}_* + r\sin\theta$, and system (5.13) is transformed into the following form:

$$\begin{cases} dr = \varepsilon f_1(r,\theta,\varepsilon)dt + \sqrt{\varepsilon} g_{11}(r,\theta,\varepsilon)dB_1(t) + \sqrt{\varepsilon} g_{12}(r,\theta,\varepsilon)dB_2(t), \\ d\theta = \varepsilon f_2(r,\theta,\varepsilon)dt + \sqrt{\varepsilon} g_{21}(r,\theta,\varepsilon)dB_1(t) + \sqrt{\varepsilon} g_{22}(r,\theta,\varepsilon)dB_2(t), \end{cases} \tag{5.14}$$

where

$$\begin{aligned} f_1(r,\theta) &= r\left((\tilde{A} + \tilde{K} - 2\tilde{K}\tilde{x}_*)\tilde{x}_* \cos^2\theta - \tilde{\alpha}\tilde{x}_* \sin\theta\cos\theta + \beta p \tilde{E}_* \sin\theta\cos\theta\right) \\ &\quad + r^2\left(-3(\tilde{K}\tilde{x}_* - \tilde{A} - \tilde{K})\cos^3\theta - \tilde{\alpha}\sin\theta\cos^2\theta + \beta p \sin^2\theta\cos\theta\right) - r^3\tilde{K}\cos^4\theta, \\ g_{11}(r,\theta) &= \tilde{\sigma}_f r\cos^2\theta, \ g_{12}(r,\theta) = \sigma_g r \sin^2\theta, \\ f_2(r,\theta) &= \left(\beta p \tilde{E}_* \cos^2\theta - (\tilde{A} + \tilde{K} - 2\tilde{K}\tilde{x}_*)\tilde{x}_* \sin\theta\cos\theta + \tilde{\alpha}\tilde{x}_* \sin^2\theta\right) \\ &\quad + r\left(\beta p \sin\theta\cos^2\theta + (3\tilde{K}\tilde{x}_* - \tilde{A} - \tilde{K})\sin\theta\cos^2\theta + \tilde{\alpha}\sin^2\theta\cos\theta\right) + r^3\tilde{K}\sin\theta\cos^3\theta, \\ g_{21}(r,\theta) &= -\tilde{\sigma}_f \sin\theta\cos\theta, \ g_{22}(r,\theta) = \sigma_g \sin\theta\cos\theta. \end{aligned}$$

According to the Khasminskii's limit theorem in [16,44], when the intensities of noise σ_f and σ_g are small and $\varepsilon \to 0$, on the time interval of ε^{-1} magnitude, the process $\{r(t), \theta(t)\}$ of system (5.14) weakly converges to a two-dimensional Markov diffusion process. Through the application of the stochastic averaging method, a stochastic differential equation as follows is obtained.

$$\begin{cases} dr = f_r(r)dt + \sigma_{11}(r)dB_r(t) + \sigma_{12}(r)dB_\theta(t), \\ d\theta = f_\theta(r)dt + \sigma_{21}(r)dB_r(t) + \sigma_{22}(r)dB_\theta(t), \end{cases} \tag{5.15}$$

where $B_r(t)$ and $B_\theta(t)$ are independent standard Wiener processes, and the coefficients of system (5.15) satisfy

$$\begin{aligned} f_r &= \varepsilon\left(\frac{(\tilde{A}+\tilde{K}-2\tilde{K}\tilde{x}_*)r\tilde{x}_*}{2} + \frac{5r}{8}(\tilde{\sigma}_f^2+\sigma_g^2) - \frac{r}{4}\tilde{\sigma}_f\sigma_g - \frac{3r^3\tilde{K}}{8}\right) \\ &= \frac{(A+K-2Kx_*)rx_*}{2} + \frac{5r}{8}(\sigma_f^2+\varepsilon\sigma_g^2) - \frac{r}{4}\sqrt{\varepsilon}\sigma_f\sigma_g - \frac{3r^3K}{8}, \\ f_\theta &= \frac{\varepsilon}{2}(\tilde{\alpha}\tilde{x}_* + \beta p\tilde{E}_*) = \frac{1}{2}(\alpha x_* + \varepsilon\beta pE_*), \\ \sigma_{12} &= \sigma_{21} = 0, \\ \sigma_{11}^2 &= \frac{3\varepsilon r^2}{8}\left(\tilde{\sigma}_f^2+\sigma_g^2+\frac{2}{3}\tilde{\sigma}_f\sigma_g\right) = \frac{3r^2}{8}\left(\sigma_f^2+\varepsilon\sigma_g^2+\frac{2}{3}\sqrt{\varepsilon}\sigma_f\sigma_g\right), \\ \sigma_{22}^2 &= \frac{\varepsilon}{8}(\tilde{\sigma}_f-\sigma_g)^2 = \frac{1}{8}(\sigma_f-\varepsilon\sigma_g)^2. \end{aligned}$$

We can easily conclude that in system (5.15), the modulus equation and phase equation are decoupled. In order to study the stability and branching phenomena of system (4.16), we only need to discuss the mean modulus equation of system (5.15), which is

$$dr = f_r(r)dt + \sigma_{11}(r)dB_r(t). \tag{5.16}$$

For convenience, we introduce the following notation:

$$c_1 = \frac{(A+K-2Kx_*)x_*}{2},\ c_2 = 5(\sigma_f^2+\varepsilon\sigma_g^2) - 2\sqrt{\varepsilon}\sigma_f\sigma_g, c_3 = 3K,\ c_4 = 3\left(\sigma_f^2+\varepsilon\sigma_g^2+\frac{2}{3}\sqrt{\varepsilon}\sigma_f\sigma_g\right).$$

Therefore, we can rewrite system (5.16) as

$$dr = \left(\left(c_1+\frac{c_2}{8}\right)r - \frac{c_4}{8}r^3\right)dt + \left(\frac{c_4}{8}r^2\right)^{\frac{1}{2}} dB_r(t). \tag{5.17}$$

We know that $r = 0$ is a fixed point of system (5.16), corresponding to the trivial solution of the original system (4.17). This section discusses the stability of the fixed points of system (5.16), as well as the stability of the singularity S_* of system (4.17).

We adopt the Lyapunov exponent method to determine the local stability of the trivial solution of system (5.17). Consider the linear Itô stochastic differential equation for system (5.17):

$$dr = \left(c_1+\frac{c_2}{8}\right)rdt + \left(\frac{c_4}{8}r^2\right)^{\frac{1}{2}} dB_r(t). \tag{5.18}$$

By utilizing the solution of Itô's stochastic differential equation, we can obtain a solution of (5.18):

$$r(t) = r(0)\exp\left\{\int_0^t \left(c_1+\frac{c_2}{8}-\frac{c_4}{16}\right)ds + \int_0^t \left(\frac{c_4}{8}\right)^{\frac{1}{2}} dB_r(s)\right\}.$$

We obtained the Lyapunov exponent of system (5.17), which is given

$$\lambda(t) = \lim_{t\to\infty} \frac{1}{t} \ln \|r(t)\| = \lim_{t\to\infty} \frac{1}{2t} \ln r(t) = \frac{1}{2}\left(c + \frac{c_2}{8} - \frac{c_4}{16}\right). \tag{5.19}$$

Therefore, the trivial solution of system (5.18) is asymptotically stable with a probability of 1, when $\lambda < 0$, i.e. $c_1 + \frac{c_2}{8} - \frac{c_4}{16} < 0$. Moreover, it has robustness against high-order random disturbances, which results in the asymptotic stability of the trivial solution of the original nonlinear system (5.17) with probability 1.

Therefore, we can obtain that:

Theorem 5.4. *If $\lambda < 0$, i.e. $c_1 + \frac{c_2}{8} - \frac{c_4}{16} < 0$, the trivial solution of system (5.17) is locally asymptotically stable with probability 1. If $\lambda > 0$, i.e. $c_1 + \frac{c_2}{8} - \frac{c_4}{16} > 0$, the trivial solution of system (5.17) is unstable. If $\lambda = 0$, i.e. $c_1 + \frac{c_2}{8} - \frac{c_4}{16} = 0$, system (5.17) may experience bifurcation.*

We use singular boundary theory to discuss the global stability of S_* of system (4.17). According to the theory of singular boundaries, when $r \to 0^+$, $\sigma_{11} = 0$, therefore $r = 0$ is the first type of singular boundary. After calculation, the diffusion index α_l, drift index β_l, and characteristic value c_l can be obtained that

$$\alpha_l = 2, \quad \beta_l = 1, \quad c_l = \lim_{r\to 0^+} \frac{2f_r(r)r^{\alpha_l-\beta_l}}{\sigma_{11}^2(r)} = \frac{16c_1 + 2c_2}{c_4}.$$

Therefore, it can be concluded that:

(a) When $c_l < 1$, i.e. $c_4 > 16c_1 + 2c_2$, the bound $r = 0$ is attractively natural;

(b) When $c_l > 1$, i.e. $c_4 < 16c_1 + 2c_2$, the bound $r = 0$ is repulsively nature;

(c) When $c_l = 1$, i.e. $c_4 = 16c_1 + 2c_2$, the bound $r = 0$ is strictly natural.

The right boundary $r = \infty$ is the second type of singular boundary, because when $r \to \infty$, $|f_r| \to \infty$. By calculation, the diffusion index $\alpha_r = 2$ and the drift index $\beta_r = 3$ can be obtained. Additionally, since $f_r(\infty) < 0$, the right boundary $r = \infty$ is an entrance boundary.

We know that all solutions of the system will enter from the right boundary and then be attracted to the left boundary, when $r = 0$ is attractively nature and $r = \infty$ is an entrance boundary. This implies that the trivial solution of system (5.17) is globally stable, which coincides with the conclusion derived by employing the Lyapunov exponent method. In other words, the trivial solution of the system is both locally and globally stable.

Therefore, we provide the following theorem:

Theorem 5.5. *The trivial solution of system (5.17) is globally stable for $c_4 > 16c_1 + 2c_2$. The trivial solution of system (5.17) is unstable for $c_4 < 16c_1 + 2c_2$. System (5.17) may undergo bifurcation for $c_4 = 16c_1 + 2c_2$.*

Remark 5.6. We refer to the method in reference [26] and transform system (4.16) into system (5.13) by introducing appropriate transformations. It should be pointed out that reference [26] uses the regular perturbation method to transform the original system into a weakly perturbed system, while the processing method in this paper differs from it. Specifically, since the system (4.16) already contains a small parameter ε, we only implement the transformation on the first equation of system (4.16). Although the transformed system (5.13) has similarities in form with weakly perturbed systems, due to significant differences in magnitude between $\tilde{f}(x, E, \varepsilon)$

and $g(x, E)$ (where $\tilde{f}(x, E, \varepsilon) = O(1/\varepsilon)$ and $g(x, E) = O(1)$), the system (5.13) still maintains typical fast-slow system characteristics. This property is mainly reflected in: There is a clear separation in the time scale of system variables; The evolution rates of fast variable x and slow variable E maintain a difference in magnitude between $O(1)$ and $O(\varepsilon)$; This conclusion differs fundamentally from the weak perturbation system obtained through regular perturbation in reference [26] in terms of mathematical properties, and also reflects the characteristics of the processing method proposed in this paper.

5.4 Stochastic bifurcation

In this section, we will study the bifurcation behavior of the system from a dynamic perspective.

Theorem 5.7. *Stochastic system* (5.17) *will generate a D-bifurcation as the value of bifurcation parameter c_4 passed through* $16c_1 + 2c_2$.

Proof. Consider the linear stochastic differential equation (5.18), which is equivalent to a Stratonovich stochastic differential equation:

$$dr = \left(c_1 + \frac{c_2}{8} - \frac{c_4}{16}\right) rdt + \left(\frac{c_4}{8} r^2\right)^{\frac{1}{2}} dB_r(t). \tag{5.20}$$

Let $m_1(r) = (c_1 + \frac{c_2}{8} - \frac{c_4}{16})r$, $\sigma_1(r) = (\frac{c_4}{8} r^2)^{\frac{1}{2}}$, system (5.20) can be rewritten as

$$dr = m_1(r)dt + \sigma_1(r)dB_r(t). \tag{5.21}$$

The continuous dynamic system generated by it is

$$\varphi(t)x = x + \int_0^t m_1(\varphi(s)x)ds + \int_0^t \sigma_1(\varphi(s)x)dB_r(s),$$

where $m_1(r) = 0$ and $\sigma_1(0) = 0$, thus 0 is a fixed point of $\varphi(x)$. Since $m_1(r)$ is bounded, the condition $\sigma_1(0) \neq 0$ is satisfied for any $m_1(r) \neq 0$, ensuring that there exists at most one stationary probability density. We have

$$\frac{\partial p}{\partial t} = -\frac{\partial}{\partial r}\left(\left(c_1 + \frac{c_2}{8}\right) p\right) + \frac{1}{2}\frac{\partial^2}{\partial r^2}\left(\left(\frac{c_4}{8} r^2\right) p\right). \tag{5.22}$$

which is the FPK equation for system (5.18).

Solving for $\frac{\partial p}{\partial t} = 0$, we obtain

$$p(r) = c \mid \sigma_1^{-1}(r) \mid \exp\left(\int_0^r \frac{2m_1(s)}{\sigma_1^2(s)} ds\right), \tag{5.23}$$

where c is constant. The system (5.22) has two possible equilibrium states: fixed point and non trivial stationary motion. The density of the invariant measure δ_0 for the former is $\delta(x)$, while the density of the invariant measure v for the latter is (5.23). As calculated, the solution for system (5.21) is

$$r(t) = r(0) \exp\left[\int_0^t (m_1'(r) + \frac{\sigma_1(r)\sigma_1''(r)}{2})ds + \int_0^t \sigma_1'(r)dB_r(s)\right]. \tag{5.24}$$

The Lyapunov exponent of a stochastic dynamical system with regard to the measure μ is

$$\lambda_{\varphi}(\mu) = \lim_{t\to\infty} \frac{1}{t} \ln \|r(t)\| \,. \tag{5.25}$$

Substitute (5.24) into(5.25), we obtain that

$$\begin{aligned}\lambda\varphi(\delta_0) &= \lim_{t\to+\infty} \frac{1}{t} \left[\ln r(0) + m_1'(0) \int_0^t ds + \sigma_1'(r) \int_0^t dB_r(s)\right] \\ &= m_1'(0) + \sigma_1'(0) \lim_{t\to+\infty} \frac{B_r(t)}{t} = m_1'(0) = c_1 + \frac{c_2}{8} - \frac{c_4}{16}.\end{aligned}$$

For the invariant measure v with a density of (5.23), the Lyapunov exponent is

$$\begin{aligned}\lambda_{\varphi}(v) &= \lim_{t\to\infty} \frac{1}{t} \int_0^t \left(m_1' + \frac{\sigma_1\sigma_1''}{2}\right)(r)ds \\ &= -32\sqrt{2}c_4^{\frac{3}{2}} \left(c_1 + \frac{c_2}{8} - \frac{c_4}{16}\right)^2 \exp\left(\frac{16}{c_4}\left(\frac{c_2}{8} - \frac{c_4}{16}\right)\right) < 0.\end{aligned}$$

In conclusion, if $c_4 > 16c_1 + 2c_2$, the fixed-point invariant measure is stable; if $c_4 < 16c_1 + 2c_2$, it is unstable; if $c_4 = 16c_1 + 2c_2$, system (5.17) undergoes a D-bifurcation. □

Theorem 5.8. *Stochastic system* (5.17) *will generate P-bifurcation as the value of bifurcation parameter* c_4 *passed through* $8c_1 + c_2$.

Proof. Based on the amplitude $r(t)$ of the stochastic differential equation, we calculate its FPK equation as follows:

$$\frac{\partial p}{\partial r} = \left\{\left((c_1 + \frac{c_2}{8})r - \frac{c_3}{8}r^3\right) p\right\} + \frac{1}{2}\frac{\partial^2}{\partial r^2}\left((\frac{c_4}{8}r^2)p\right),$$

whose initial condition is

$$p(r,t|r_0,t_0) \to \delta(r - r_0), \quad t \to t_0,$$

where $p(r,t|r_0,t_0)$ represents the transition probability density of the diffusion process $r(t)$. The invariant measure of $r(t)$ is the steady-state probability density function $p_{st}(r)$, which serves as the solution to the following degenerate system:

$$-\frac{\partial}{\partial r}\left\{\left(\left(c_1 + \frac{c_2}{8}\right) r - \frac{c_3}{8}r^3\right) p\right\} + \frac{1}{2}\frac{\partial^2}{\partial r^2}\left(\frac{c_4}{8}r^2\right) p = 0.$$

By calculation, it can be concluded that

$$p_{st}(r) = \begin{cases} \dfrac{r^{\frac{16c_1+2c_2-2c_4}{c_4}} e^{-\frac{c_3}{c_4}r^2}}{\Gamma\left(\frac{8c_1+c_2}{c_4}\right)\left(\frac{c_4}{c_3}\right)^{\frac{8c_1+c_2}{c_4}}}, & c_4 < 16c_1 + 2c_2, \\ \delta_0, & c_4 \geq 16c_1 + 2c_2. \end{cases} \tag{5.26}$$

According to Namachivaya's theory, the extremum of invariant measures can explain the key characteristics of correlated nonlinear stochastic systems. If r_* represents the maximum value point of $p_{st}(r)$, the sample trajectory is likely to remain in the vicinity of r_* with a high probability, suggesting that r_* is stable in a probabilistic sense. Conversely, if $p_{st}(r)$ has a minimum value, the situation is reversed.

To solve for the extremum of $p_{st}(r)$, we need to solve the following equation:

$$\frac{\left(\frac{16c_1+2c_2-2c_4}{c_4} - \frac{2c_3}{c_4}r^2\right) r^{\frac{16c_1+2c_2-3c_4}{c_4}} e^{-\frac{c_3}{c_4}r^2}}{\Gamma\left(\frac{8c_1+c_2}{c_4}\right)\left(\frac{c_4}{c_3}\right)^{\frac{8c_1+c_2}{c_4}}} = 0.$$

By simple calculation, we obtain $r = 0$ or $r_* = \sqrt{\frac{8c_1+c_2-c_4}{c_3}}$. The system reaches its maximum value at r_* if $c_4 < 8c_1 + c_2$. Therefore, we can prove the following three situations:

Case (i): If $8c_1 + c_2 < c_4 < 16c_1 + 2c_2$ and $r \to 0^+$, $p_{st}(r)$ tends to infinity. At this time, the sample trajectory of the system is concentrated around $r = 0$.

Case (ii): If $\frac{16c_1+2c_2}{3} < c_4 < 8c_1 + c_2$, $p_{st}(r)$ attains its maximum at $r = r_*$ and its minimum at $r = 0$. However, $p_{st}(r)$ is not differentiable at $r = 0$ in this scenario.

Case (iii): If $c_4 < \frac{16c_1+2c_2}{3}$, $p_{st}(r)$ attains its maximum at $r = r_*$ and its minimum at $r = 0$. At this time, $p_{st}(r)$ is differentiable at $r = 0$, and it is easy to find that $p_{st}(r)$ is smooth at $r = 0$.

Based on the above analysis, we know that the shape of $p_{st}(r)$ will change from a monotonic to a unimodal as the c_4 value exceeds $8c_1 + c_2$. System (5.17) generates a stochastic P-bifurcation if $c_4 = \frac{16c_1+2c_2}{3}$. □

Remark 5.9. The sample trajectory of the system is concentrated around $r = 0$ for $8c_1 + c_2 < c_4 < 16c_1 + 2c_2$, indicating a high probability of a small population size, which is not conducive to population growth. As c_4 decreases, the peak value of $p_{st}(r)$ narrows and shifts to the right (see Figure 5.2(a) and Figure 5.2(b)), indicating a higher probability of a larger population size, which is beneficial for population growth.

5.5 Numerical simulation

In this section, we will use data simulation to verify the correctness of the above theory.

We select parameter $K = 3$, $A = -0.8$, $\alpha = 0.17$, $\varepsilon = 0.1$, $\beta = 1.5$, $p = 3$, $c = 1.69$, $\sigma_f = 0.001$ and $\sigma_g = 0.001$ and $\sigma_g = 0.001$ in system (4.17), which satisfy the conditions

$$\frac{\varepsilon(A + \frac{\sigma_f^2}{2})}{\alpha} < \frac{c + \frac{\sigma_g^2}{c}}{c}, \quad \varepsilon < \alpha c \quad \text{and} \quad \beta p < \frac{1}{\varepsilon}$$

(the data source from Table 3.2.). According to Theorem 5.2, it is known that system (4.17) has a stationary distribution. In a sense, it also indicates that small-scale noise is beneficial for system stability. As shown in Figure 5.1. The values of $x(t)$ and $E(t)$ in Figure 5.1(a) and Figure 5.1(c) oscillate slightly around the equilibrium point of the deterministic system. The bar charts in Figure 5.1(b) and Figure 5.1(d) show that system (4.17) exhibits a stationary distribution.

Next, we will verify the conclusion of stochastic bifurcation through numerical simulation. We select parameters $c_1 = 0.25$, $c_2 = 3$, $c_3 = 10$ and $c_4 = 5$ so that they satisfy the case (i) in the proof of Theorem 5.8. Figure 5.2 shows the stationary probability density $p_{st}(r)$ of system (5.17), from which we can see that $p_{st}(r)$ tends towards infinity when $r \to 0^+$.

We select parameters $c_1 = 0.25$, $c_2 = 3$, $c_3 = 10$ and $c_4 = 3.5$ so that they satisfy the case (ii). Figure 5.3 shows the graph of $p_{st}(r)$, from which we can see that $p_{st}(r)$ reaches its maximum at $r = r_*$ and its minimum at $r = 0$.

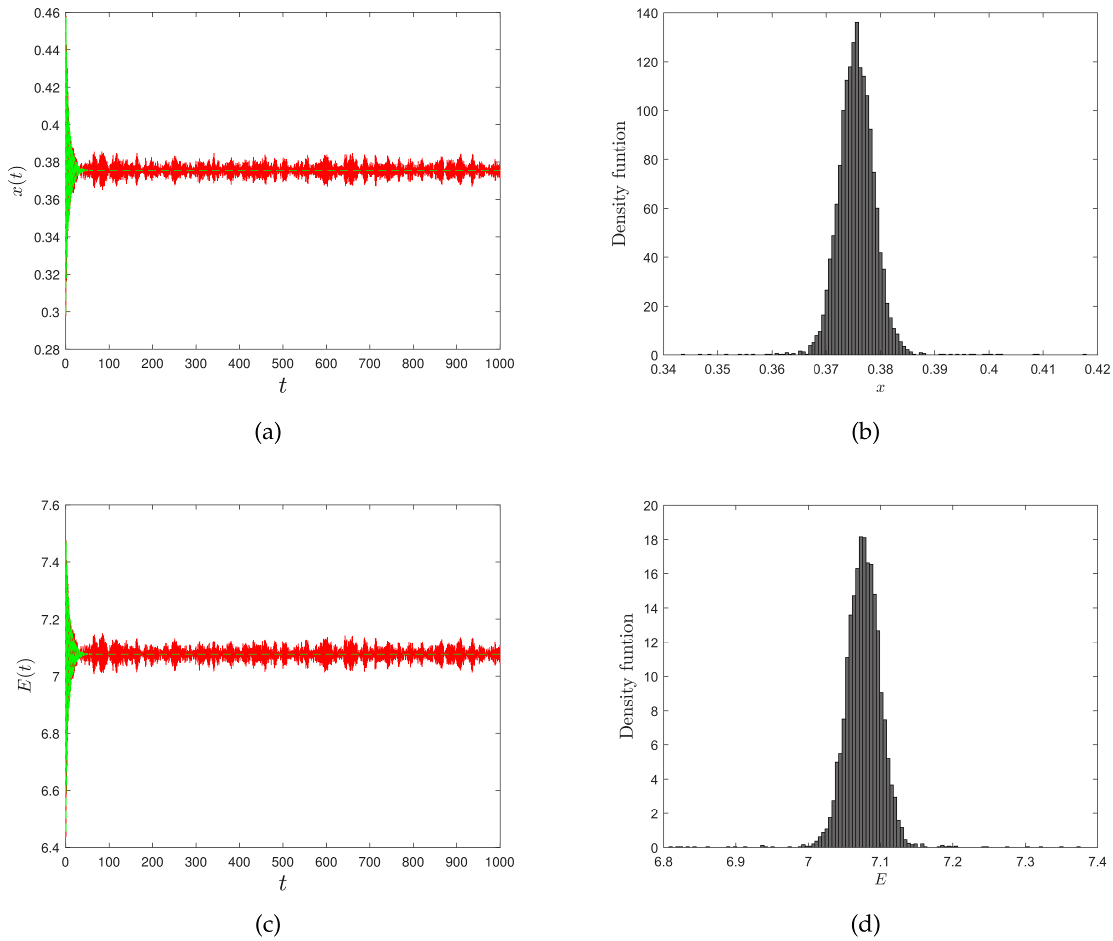

Figure 5.1: (a,c): Comparison of the solutions $x(t)$ and $E(t)$ of system (4.17) with the corresponding deterministic system solutions. The red line stands for the solution of the stochastic system, and the green line stands for the solution of the corresponding deterministic system. (b,d): The histogram of the probability density functions of x, E populations.

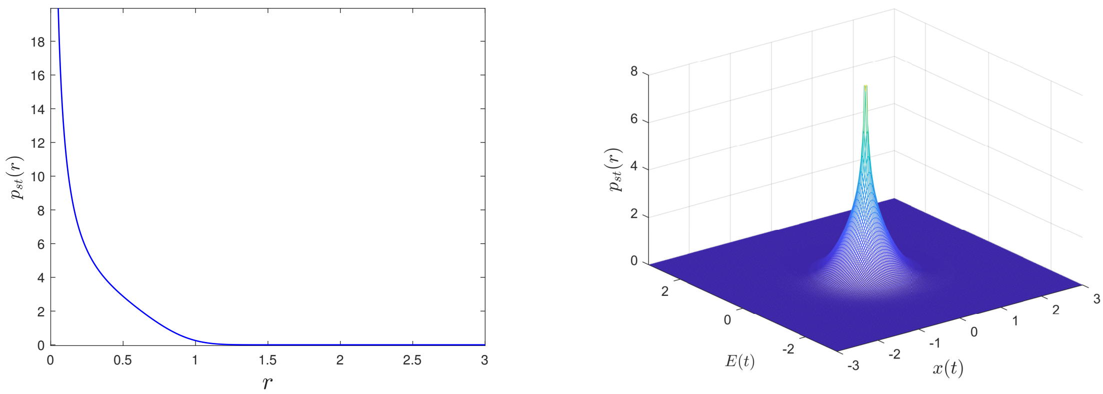

(a) (b)

Figure 5.2: The stationary probability density $p_{st}(r)$ of system (5.17) with $c_1 = 0.25$, $c_2 = 3$, $c_3 = 10$ and $c_4 = 5$.

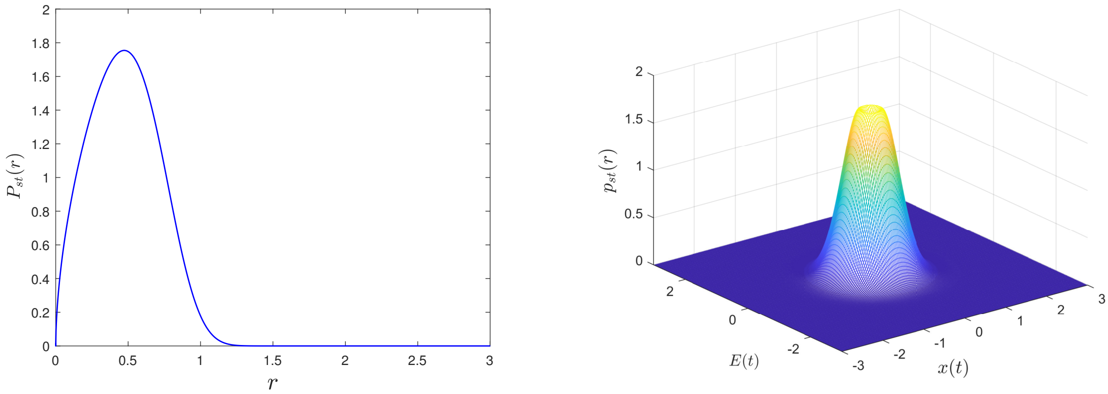

(a) (b)

Figure 5.3: The stationary probability density $p_{st}(r)$ of system (5.17) with $c_1 = 0.25$, $c_2 = 3$, $c_3 = 10$ and $c_4 = 3.5$.

We select parameters $c_1 = 0.25$, $c_2 = 3$, $c_3 = 10$ and $c_4 = 2$ so that they satisfy the case (iii). Figure 5.4 shows the graph of $p_{st}(r)$, from which we can see that $p_{st}(r)$ reaches its maximum at $r = r_*$ and its minimum at $r = 0$.

We compare the effects of noise intensity σ_f and σ_g on the peak value of probability density $p_{st}(r)$ under strong and weak Allee effect. Selecting parameter $K = 3$, $A = 0.2$, $\alpha = 0.2$, $\varepsilon = 0.9$, $\beta = 1.1$, $p = 2.5$, $c = 1$, $\sigma_g = 0.7$ and $K = 3$, $A = -0.2$, $\alpha = 0.2$, $\varepsilon = 0.9$, $\beta = 1.1$, $p = 2.5$, $c = 1$, $\sigma_g = 0.7$, we plotted the graph of peak versus σ_f(see Figure 5.5(a)). Selecting parameter $K = 3$, $A = 0.2$, $\alpha = 0.2$, $\varepsilon = 0.9$, $\beta = 1.1$, $p = 2.5$, $c = 1$, $\sigma_f = 0.7$ and $K = 3$, $A = -0.2$, $\alpha = 0.2$, $\varepsilon = 0.9$, $\beta = 1.1$, $p = 2.5$, $c = 1$, $\sigma_f = 0.7$, we plotted the graph of peak versus σ_g(see Figure 5.5(b)). From the graph, we can observe that as the values of σ_f and σ_g increase, the peak value of $p_{st}(r)$ first increases and then decreases, indicating that the survival probability of the population will be higher under appropriate noise intensity. This is also consistent with reality, indicating that moderate harsh environments can promote

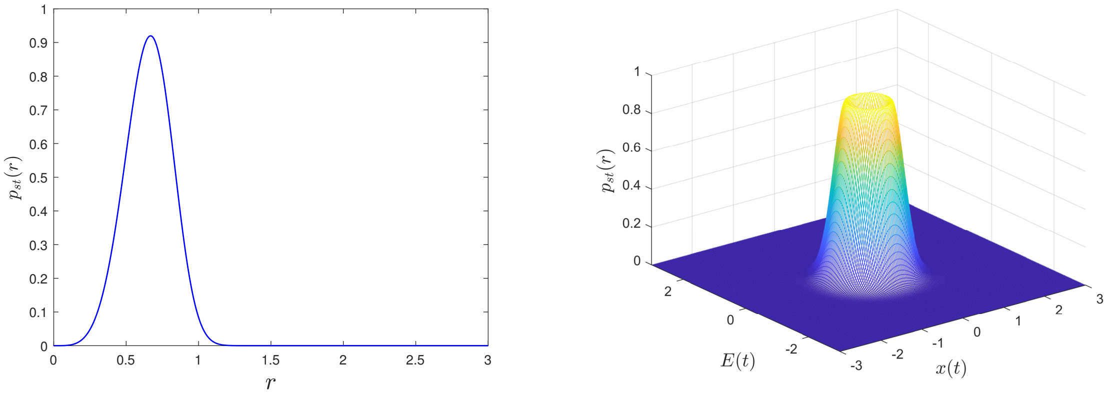

(a) (b)

Figure 5.4: The stationary probability density $p_{st}(r)$ of system (5.17) with $c_1 = 0.25$, $c_2 = 3$, $c_3 = 10$ and $c_4 = 2$.

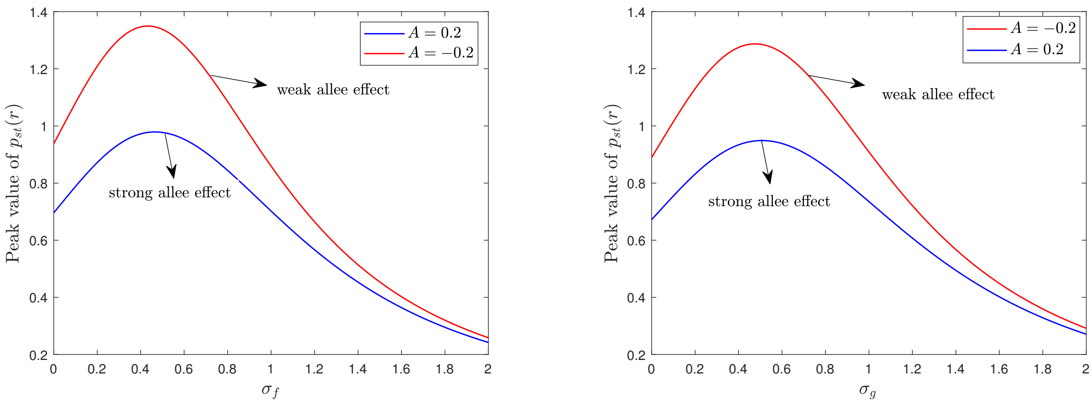

(a) (b)

Figure 5.5: (a) The effect of parameter σ_f on the peak value of $p_{st}(r)$. (b) The effect of parameter σ_g on the peak value of $p_{st}(r)$.

the reproduction of biological populations, while extreme natural environments can lead to the extinction of organisms. From Figure 5.5, it can also be observed that the probability of population survival under weak Allee effects is higher than that under strong Allee effects.

Finally, we discuss the impact of random noise on relaxation oscillations [1] through numerical simulation. Choosing parameter $K = 2$, $A = -0.5$, $\alpha = 0.17$, $\varepsilon = 0.01$, $\beta = 0.4$, $p = 1$, $c = 0.14$, $\sigma_f = 0.02$ and $\sigma_g = 0.02$, We have plotted the influence diagram noise on relaxation oscillation (see Figure 5.6). We found that noise will fluctuate near the relaxation oscillation, that is, the noise will approximately stabilize near the relaxation oscillation of deterministic system.

Remark 5.10. Environmental fluctuations highlight the importance of ecosystem protection. The fishery bioeconomic model can help evaluate the role of ecosystem conservation measures in responding to environmental fluctuations. For example, after setting up a marine protected area in a fishing ground, during environmental fluctuations, the fish population

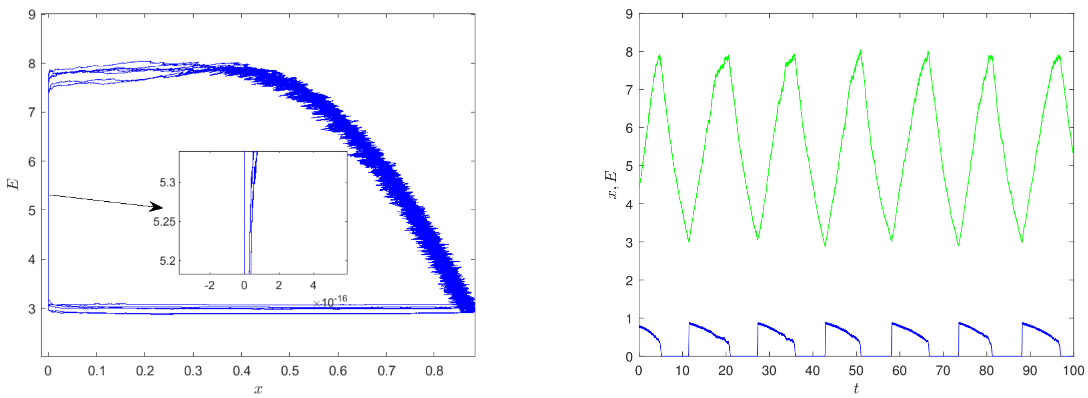

(a) (b)

Figure 5.6: (a) The influence diagram noise on relaxation oscillation. (b) $x - t$ (blue) and $E - t$ (green) time series diagram.

within the protected area may serve as a "source" to provide juvenile fish supplements to surrounding fishing grounds, thereby maintaining the stability of the entire fishing ecosystem. Fishery managers also need to adjust their fishing strategies based on environmental fluctuations. During periods of significant environmental fluctuations, stricter fishing restrictions may be necessary, such as reducing fishing quotas and extending fishing bans. This is because environmental fluctuations have already caused natural pressure on fish populations, and overfishing may make it difficult for populations to recover, leading to the depletion of fishery resources. The fishery bioeconomic model can simulate the effects of different fishing strategies under environmental fluctuations, providing scientific decision-making basis for managers.

6 Conclusion

This paper investigates the bifurcation behavior of a class of stochastic fast slow single population fishery economic models with Allee effect.

For the deterministic fast-slow system (2.2) with strong Allee effect, we studied the fast-slow dynamic behavior of the system and revealed that as the bifurcation parameters change, the system produces stable canard circle, which happen to coincide with the Hopf bifurcation of the normal system. Compared to the strong Allee effect, for deterministic fast-slow systems (2.2) with weak Allee effect, more complex dynamic properties will be generated, not only canard circle, but also a fast-slow periodic cycle (relaxation oscillation). The existence of canard circle and relaxation oscillations indicates that the system will have a periodic oscillation, which means that the system is in dynamic equilibrium. For the aquaculture industry, it is beneficial for fishermen to optimize resource allocation and sustain economic turnover.

For the stochastic fast-slow fishery economic system, we discussed the existence of a stationary distribution for the system (4.18)after stochastic reduction. And with the time scale parameter as a general parameter, we studied the existence of stationary distribution and stochastic bifurcation behavior of the system (4.17). We conclude that both strong Allee effect and weak Allee effect, the system system (4.18) has a stationary distribution, and as the bifurcation parameter c_4 changes, stochastic P-bifurcation and stochastic D-bifurcation will occur. Then we compared the changes in peak density of stationary distributions under different Allee effects, and concluded that under the same noise influence, weak Allee effects are more conducive to population survival (see Figure 5.5). Using the image (Figure 5.6) to describe the effect of the time scale parameter c on relaxation oscillations, we found that random fluctuations tend to stabilize near relaxation oscillations.

On the basis of this article, there is still relevant work that can be further studied. In this article, we only considered single population models, and in the future, we can study the relevant properties and bifurcation studies of multiple population models, as well as the bifurcation behavior of systems at multiple time scales.

Appendix

We provide a proof of convergence for the integrals $I_1 = \int_{x(0)}^{+\infty} x^{-N} \exp\left\{\frac{2(K+A)}{\sigma_f^2}x - \frac{K}{\sigma_f^2}x^2\right\}dx$ and $I_2 = \int_{x(0)}^{+\infty} x^{-N+1} \exp\left\{\frac{2(K+A)}{\sigma_f^2}x - \frac{K}{\sigma_f^2}x^2\right\}dx$.

Let $u = \frac{x}{\sigma_f}$, we obtain

$$
\begin{aligned}
I_1 &= \sigma_f^{-N+1} \int_{x(0)}^{+\infty} u^{-N} \exp\left\{-Ku^2 + \frac{2(K+A)u}{\sigma_f}\right\} du \\
&= \sigma_f^{-N+1} e^{\frac{(K+A)^2}{K\sigma_f^2}} \int_{x(0)}^{+\infty} u^{-N} \exp\left\{-K\left(u - \frac{K+A}{K\sigma_f}\right)^2\right\} du, \quad \text{taking } y = u - \frac{K+A}{K\sigma_f}, \\
&= \sigma_f^{-N+1} e^{\frac{(K+A)^2}{K\sigma_f^2}} \int_{x(0)-\frac{K+A}{K\sigma_f}}^{+\infty} \left(y + \frac{K+A}{K\sigma_f}\right)^{-N} e^{-Ky^2} dy.
\end{aligned}
$$

By calculation, we can conclude that e^{-Ky^2} is monotonically decreasing and bounded on the interval $(x(0) - \frac{K+A}{K\sigma_f}, +\infty)$. Since $N > 2$, we can obtain that

$$
\int_{x(0)-\frac{K+A}{K\sigma_f}}^{+\infty} \left(y + \frac{K+A}{K\sigma_f}\right)^{-N} dy = \int_{x(0)}^{+\infty} u^{-N} du,
$$

is convergent. Therefore, according to the Abel convergence criterion, we conclude that the integral I_1 is convergent. Similarly, we can also conclude that I_2 converges.

Acknowledgment

This research was supported by National Natural Science Foundation of China (61703083) and Regional joint key project of National Natural Science Foundation (U23A20324).

References

[1] X. Ai, Y. Zhang, Dynamic analysis of phytoplankton-zooplankton-fish singular perturbation system on three time-scales, *Chaos Solitons Fractals* **190**(2025), 115711. https://doi.org/10.1016/j.chaos.2024.115711

[2] T. K. Ang, H. M. Safuan, H. S. Sidhu, Z. Jovanoski, I. N. Towers, Impact of harvesting on a bioeconomic predator–prey fishery model subject to environmental toxicant, *Bull. Math. Biol.* **81**(2018), No.7, 2748–2767. https://doi.org/10.1007/s11538-019-00627-8; MR3977632; Zbl 1417.92122

[3] H. Boudjellaba, T. Sari, Dynamic transcritical bifurcations in a class of slow-fast predator-prey models, *J. Differential Equations* **246**(2009), No. 6, 2205–2225. https://doi.org/10.1016/j.jde.2009.01.001; MR2498839; Zbl 1284.34096

[4] C. Chai, Y. Shao, Y. Wang, Analysis of a Holling-type IV stochastic prey–predator system with anti-predatory behavior and Levy noise, *AIMS Math.* **8**(2023), No. 9, 21033–21054. https://doi.org/10.3934/math.20231071; MR4618555

[5] K. Chakraborty, T. K. Kar, Economic perspective of marine reserves in fisheries: A bioeconomic model, *Math. Biosci.* **240**(2012), No. 2, 212–222. https://doi.org/10.1016/j.mbs.2012.07.008; MR3000373; Zbl 1316.91023

[6] P. R. Chowdhury, M. Banerjee, S. Petrovskii, Canards, relaxation oscillations, and pattern formation in a slow-fast ratio-dependent predator–prey system, *Appl. Math. Model.* **31**(2022), 519–535. https://doi.org/10.1016/j.apm.2022.04.022; MR4426012; Zbl 1505.92150

[7] C. W. Clark, *Mathematical bioeconomics. The optimal management of renewable resources*, John Wiley & Sons, New York, 1990. https://doi.org/10.2307/2830861; MR0416658; Zbl 0712.90018

[8] P. De Maesschalck, S. Schecter, The entry-exit function and geometric singular perturbation theory, *J. Differential Equations* **260**(2016), No. 8, 6697–6715. https://doi.org/10.1016/j.jde.2016.01.008; MR3460228; Zbl 1342.34078

[9] N. Fenichel, Geometric singular perturbation theory for ordinary differential equations, *J. Differential Equations* **31**(1979), No. 1, 53–98. https://doi.org/10.1016/0022-0396(79)90152-9; MR0524817; Zbl 0476.34034

[10] X. Gao, Y. Zhang, Bifurcation analysis and optimal control of a delayed single-species fishery economic model, *Math. Biosci. Eng.* **19**(2022), No. 8, 8081–8106. https://doi.org/10.3934/mbe.2022378; MR4437584; Zbl 1508.91397

[11] M. J. Groom, Allee effects limit population viability of an annual plant, *Am. Nat.* **151**(1998), No. 61, 487–496. https://doi.org/10.1086/286135

[12] B. Han, D. Jiang, Threshold dynamics and probability density functions of a stochastic predator–prey model with general distributed delay, *Commun. Nonlinear Sci. Numer. Simul.* **128**(2024), 107596. https://doi.org/10.1016/j.cnsns.2023.107596; MR4655643; Zbl 1531.34075

[13] D. Huang, H. Wang, J. Feng, Z. Zhu, Hopf bifurcation of the stochastic model on HAB nonlinear stochastic dynamics, *Chaos Solitons Fractals* **27**(2006), No. 4, 1072–1079. https://doi.org/10.1016/j.chaos.2005.04.086; MR2166689; Zbl 1134.34312

[14] Z. Huang, Q.-G. Yang, J. Cao, The stochastic stability and bifurcation behavior of an internet congestion control model, *Math. Comput. Modelling* **54**(2011), No. 9–10, 1954–1965. https://doi.org/10.1016/j.mcm.2011.05.002; MR2834601; Zbl 1235.93250

[15] J. Jiang, X. Li, X. Wu, The dynamics of a bioeconomic model with Michaelis–Menten type prey harvesting, *Bull. Malays. Math. Sci. Soc.* **46**(2023), No. 2, 57. https://doi.org/10.1007/s40840-022-01452-4; MR4530219; Zbl 1512.34095

[16] R. Z. Khasminskii, A limit theorem for the solution of differential equations with random right-hand sides, *Theory Probab. Appl.* **11**(1966), No. 3, 390–406. https://doi.org/10.1137/1111038

[17] R. Z. Khasminskii, On transition densities of singularly perturbed diffusions with fast and slow components, *SIAM J. Appl. Math.* **56**(1996), No. 6, 1794–1819. https://doi.org/10.1137/S0036139995282906; Zbl 0863.60076

[18] A. M. Kramer, B. Dennis, A. M. Liebhold, J. M. Drake, The evidence for Allee effects, *Popul. Ecol.* **51**(2009), No. 3, 341–354. https://doi.org/10.1007/s10144-009-0152-6

[19] C. Kuehn, *Multiple time scale dynamics*, Springer, Cham, 2015. https://doi.org/10.1007/978-3-319-12316-5; MR3309627 ;Zbl 1335.34001

[20] S. Li, Incorporation of fisheries policy into regional blocs? – Lessons from the EU's common fisheries policy, *Fishes* **7**(2022), No. 3, 102. https://doi.org/10.3390/fishes7030102

[21] S. Li, C. Wang, K. Wu, Relaxation oscillations of a slow-fast predator–prey model with a piecewise smooth functional response, *Appl. Math. Lett.* **113**(2021), 106852. https://doi.org/10.1016/j.aml.2020.106852; MR4168274; Zbl 1457.92144

[22] Z. Li, Y. Zhang, Dynamic analysis of a fast slow modified Leslie–Gower predator–prey model with constant harvest and stochastic factor, *Math. Comput. Simulation* **226**(2024), 474–499. https://doi.org/10.1016/j.matcom.2024.07.027; MR4778253

[23] Q. Lin, Stability analysis of a single species logistic model with Allee effect and feedback control, *Adv. Difference Equ.* **2018**, Paper No. 190. https://doi.org/10.1186/s13662-018-1647-2; MR3804093; Zbl 1446.92225

[24] T. Liu, L. Chen, F. Chen, Z. Li, Dynamics of a Leslie–Gower model with weak Allee effect on prey and fear effect on predator, *Int. J. Bifurcation Chaos Appl. Sci. Eng.* **33**(2023), No. 1, 2350008. https://doi.org/10.1142/S0218127423500086; MR4546896; Zbl 1543.92043

[25] W. Liu, Y. Jiang, Bifurcation of a delayed Gause predator–prey model with Michaelis–Menten type harvesting, *J. Theor. Biol.* **438**(2018), 116–132. https://doi.org/10.1016/j.jtbi.2017.11.007; MR3734372; Zbl 1394.92109

[26] C. Luo, S. Guo, Stability and bifurcation of two-dimensional stochastic differential equations with multiplicative excitations, *Bull. Malays. Math. Sci. Soc.* **40**(2017), No. 2, 795–817. https://doi.org/10.1007/s40840-016-0313-7; MR3620282; Zbl 1365.34103

[27] A. Maurya, A. Priyadarshi, Fish harvesting strategies with allee effect, *ITM Web Conf.* **34**(2020), 02004. https://doi.org/10.1051/itmconf/20203402004

[28] G. Merino, F. Maynou, Effort dynamics in a fisheries bioeconomic model: A vessel level approach through game theory, *Sci. Mar.* **71**(2007), No. 3, 537–550. https://doi.org/10.3989/scimar.2007.71n3537

[29] C. B. Muratov, E. Vanden-Eijnden, Noise-induced mixed-mode oscillations in a relaxation oscillator near the onset of a limit cycle, *Chaos* **18**(2008), No. 1, 015111. https://doi.org/10.1063/1.2779852; MR2404667

[30] L. Perko, *Differential equations and dynamical systems*, 3rd ed., Springer, New York, 2001. https://doi.org/10.1007/978-1-4613-0003-8; Zbl 0973.34001

[31] T. Saha, P. J. Pal, M. Banerjee, Relaxation oscillation and canard explosion in a slow-fast predator–prey model with Beddington–DeAngelis functional response, *Nonlinear Dyn.* **103**(2021), No. 1, 1195–1217. https://doi.org/10.1007/s11071-020-06140-1; MR3621236; Zbl 1516.92094

[32] J. Shen, Canard limit cycles and global dynamics in a singularly perturbed predator–prey system with non-monotonic functional response, *Nonlinear Anal.* **31**(2016), 146–165. https://doi.org/10.1016/j.nonrwa.2016.01.013; MR3490837; Zbl 1375.92056

[33] M. D. Smith, J. N. Sanchirico, J. E. Wilen, The economics of spatial-dynamic processes: Applications to renewable resources, *J. Environ. Econ. Manage.* **57**(2009), No. 1, 104–121. https://doi.org/10.1016/j.jeem.2008.08.001; Zbl 1159.91439

[34] H. J. Tidbury, A. Muench, P. D. Lamb, K. Hyder, Balancing biological and economic goals in commercial and recreational fisheries: systems modelling of sea bass fisheries, *ICES J. Mar. Sci.* **78**(2021), No. 5, 1793—1803. https://doi.org/10.1093/icesjms/fsab087

[35] E. Vercken, A. M. Kramer, P. C. Tobin, J. M. Drake, Critical patch size generated by Allee effect in gypsy moth, *Lymantria dispar* (L.), *Ecol. Lett.* **14**(2011), No. 2, 179–186. https://doi.org/10.1111/j.1461-0248.2010.01569.x

[36] H. Wang, Phenomenological bifurcation in a generally stochastic population model with Allee effect, *Eur. Phys. J. E* **45**(2022), No. 10, 87. https://doi.org/10.1140/epje/s10189-022-00235-w

[37] C. Wang, X. Zhang, Stability loss delay and smoothness of the return map in slow-fast systems, *SIAM J. Appl. Dyn. Syst.* **17**(2018), No. 1, 788–822. https://doi.org/10.1137/17M1130010; MR3777397; Zbl 1396.34042

[38] T. Wen, Y. Xu, M. He, L. Rong, Modelling the dynamics in a predator-prey system with Allee effects and anti-predator behavior, *Qual. Theory Dyn. Syst.* **22**(2023), No. 3, 116. https://doi.org/10.1007/s12346-023-00821-z;MR4600292;Zbl 1519.34052

[39] J. Wiedenmann, J. Wilen, P. Levin, M. Plummer, M. Mangel, A framework for exploring the role of bioeconomics on observed fishing patterns and ecosystem dynamics, *Coast. Manage.* **44**(2016), No. 5, 529–546. https://doi.org/10.1080/08920753.2016.1208886

[40] F. Wu, G. Yin, An averaging principle for two-time-scale stochastic functional differential equations, *J. Differential Equations* **269**(2020), No. 1, 1037–1077. https://doi.org/10.1016/j.jde.2019.12.024; MR4081541; Zbl 1442.34127

[41] X. Yu, Y. Ma, Noise-induced dynamics in a single species model with Allee effect driven by correlated colored noises, *J. Theor. Biol.* **573**(2023), 111610. https://doi.org/10.1016/j.jtbi.2023.111610; MR4632756; Zbl 1521.92079

[42] Y. Zhang, X. Wu, Dynamic behavior and sliding mode control on a stochastic epidemic model with alertness and distributed delay, *Commun. Nonlinear Sci. Numer. Simul.* **124**(2023), 107299. https://doi.org/10.1016/j.cnsns.2023.107299; MR4593969; Zbl 1523.37101

[43] W. Zhang, M. Zhao, Spatiotemporal dynamics of phytoplankton-fish system with the Allee effect and harvest effect, *Adv. Mater. Res.* **726–731**(2013), 1604–1610. https://doi.org/10.4028/www.scientific.net/AMR.726-731.1604

[44] W. Zhu, *Nonlinear dynamics and control Hamilton theoretical system frame*, Science Press, Beijing, 2003.